Coexistence Analysis for Multiple Air-to-Ground Systems

Dr. Anthony A. Triolo
Dr. Jay E. Padgett
Telcordia Technologies, Inc.
Applied Research
Wireless Systems and Networks

June 3, 2004

Executive Summary

This technical paper evaluates analyses submitted to the Federal Communications Commission in WT Docket No. 03-103 concerning two competing proposals for accommodating multiple broadband service providers in the Air-to-Ground (ATG) service – the "AirCell and Boeing Proposals." ATG uses spectrum in the 849-851 MHz and 894-896 MHz bands. The aircraft receives on the low band and transmits on the high band. The current band plan uses 6 kHz channels and supports narrowband transmissions only, primarily speech. Verizon Airfone, the only remaining service provider using the ATG bands, has proposed a modification of the Commission's technical rules to support a broadband approach that will permit a single 1.25 MHz wideband channel in each direction. The intent is to support data-centric applications such as e-mail and web browsing. The 1.25 MHz bandwidth specification will allow the use of technologies developed for terrestrial mobile radio services.

AirCell has proposed a scheme to support sharing of the ATG bands by two separate service providers, each having access to a 1.25 MHz block in each direction. AirCell's proposal is to reverse the duplexing for the second provider, so its aircraft would receive in the 895 MHz band and transmit in the 850 MHz band. Alternatively, Boeing has suggested the use of adaptive antennas on all aircraft and base stations to alleviate the interference problems associated with multiple, broadband use of ATG spectrum.

AirCell Proposal. AirCell's analysis of its proposal is deficient in four major respects:

(1) AirCell relies on textbook assumptions for equipment performance and propagation, with no allowance or sensitivity analysis to account for imperfections such as fading, errors in antenna alignment, and equipment implementation losses;

(2) AirCell fails to consider the harmful effects of base-to-base station interference that would undoubtedly occur with reversed duplexing;

(3) AirCell severely underestimates aircraft-to-aircraft interference because its analysis does not reflect real-world conditions;

(4) AirCell's analysis artificially constrains the maximum aircraft transmit power to two-tenths of a watt (equivalent to a single cellular or PCS handset), resulting in the understated aircraft-to-aircraft interference potential it reports; and

(5) AirCell fails to consider the overwhelming interference effects of the adjacent channel AN/SPS-49 air search radar systems deployed by the U.S. Navy.

It is shown here, using a simple simulation similar to AirCell's, that as a result of these flaws in the AirCell analysis, it significantly underestimates the harmful interference effects associated with reverse-duplexed sharing of the ATG spectrum. Following that, an extensive simulation is developed which takes into account a number of real-world factors that AirCell omitted including: (1) non-uniform geographical distribution of air traffic; (2) sectorized base station antenna patterns; (3) sectorized antennas on the victim aircraft with a best-beam selection system; and (4) actual existing base station locations. When the AirCell proposal is appropriately modeled in this fashion, it is clear that the harmful interference effects on each of the two ATG broadband systems are significant despite the mitigation measures incorporated into the simulation. Moreover, base-to-base interference will be present in most airport environments, which would have a debilitating effect on the operation of the ATG service. Finally, the Navy radar system will severely impact the communication ability of a reverse-duplexed system.

The conclusion is that a reverse-duplex arrangement for spectrum sharing is not viable in the ATG spectrum.

Boeing Proposal. Technical analysis of this proposal demonstrates that for the configuration proposed by Boeing:

(1) Reasonably sized adaptive antennas cannot eliminate harmful interference between multiple broadband providers in the ATG spectrum;

(2) The adaptive array system will add significant size, weight and power consumption requirements and will therefore not be practical in an aviation environment; and

(3) There are no commercially available off-the-shelf adaptive array systems for ATG broadband communications applications, and the development and production of such systems would significantly delay bringing a broadband ATG service to market.

Boeing's analysis fails to consider typical airport environments and aircraft flight patterns. When studying such real-world situations through use of a simulation, it is clear that massive adaptive antenna arrays mounted on the aircraft belly would be necessary to avoid harmful interference with multiple, frequency overlapping ATG systems. The use of such arrays in an ATG system is impractical. Even if a reasonably sized array could

be developed to eliminate the interference effects associated with the Boeing proposal, the complexity and time-to-market delays associated with developing such technology would make such a system fail to be commercially viable.

The conclusion is that the use of belly-mounted adaptive array antenna systems is not an effective solution for the interference that would result from multiple, frequency overlapping ATG systems.

Table of Contents

1. Introduction 5
2. The AirCell Simulation Framework 9
   2.1. Overview of the AirCell Simulation 9
   2.2. Comments on the AirCell Model 10
      2.2.1. Minor Observations 10
      2.2.2. Major Deficiencies 11
3. Square-Grid Simulation 13
   3.1. General Description 13
   3.2. Link Budgets 14
   3.3. Outer-Cell Forward Link Interference 17
   3.4. Simulation Variations and Results 19
   3.5. Average Rate, Outage Probability, and Sensitivity to Simulation Mechanics . 25
   3.6. Comparison of Simulation Results with Analytical Approximation 29
4. Simulation of Cross-Duplexed Systems under "Real World" Conditions 31
   4.1. Introduction 31
   4.2. Air traffic density and distribution modeling 32
   4.3. Victim Network Characteristics 36
   4.4. Interfering Network Characteristics 39
   4.5. Simplified Interference Example 43
   4.6. Monte Carlo Simulation Methodology 44
   4.7. Results 46
   4.8. Conclusions 51
5. Effect of Naval Air-Search Radars on Reverse-Duplexed Aircraft Reception 53
6. Adaptive Antenna Issues for Multiple System Coexistence 54
   6.1. Introduction 54
   6.2. System Layout 55
   6.3. Antenna Size Considerations 56
   6.4. System Complexity Considerations 60
   6.5. Conclusions 61
7. Annex A: The Radio Horizon 63
8. Annex B: Reverse Link Capacity and Load Factor 64
9. Annex C: Analytical Approximation of the SIR Using Circular Geometry 68
10. References 78

1. Introduction

The bands 849-851 MHz and 894-896 MHz are allocated to Air-to-Ground (ATG) communication. The aircraft receives on the low band and transmits on the high band.[1] The current band plan uses 6-kHz channels and supports narrowband transmissions, primarily speech. Verizon Airfone, the only remaining service provider using the ATG bands, has proposed modification of the band plan to support a broadband approach which will require a single 1.25-MHz wideband channel in each direction [1]. The intent is to support data-centric applications such as e-mail and web browsing while continuing to provide voice service as part of its broadband offering.

AirCell has proposed a scheme to support sharing of the ATG bands by two separate service providers, each having access to 1.25 MHz of the 2 MHz of ATG spectrum available in each direction (so frequency overlap is unavoidable). AirCell's proposal is to invert the duplexing for the second provider, so its aircraft would receive on the high band and transmit on the low band. This means that the transmissions from the aircraft of provider 1 could interfere with the reception on the aircraft of provider 2, and vice versa. The same is true of base stations if their separation is less than the radio horizon. Figure 1 illustrates the interference between aircraft.

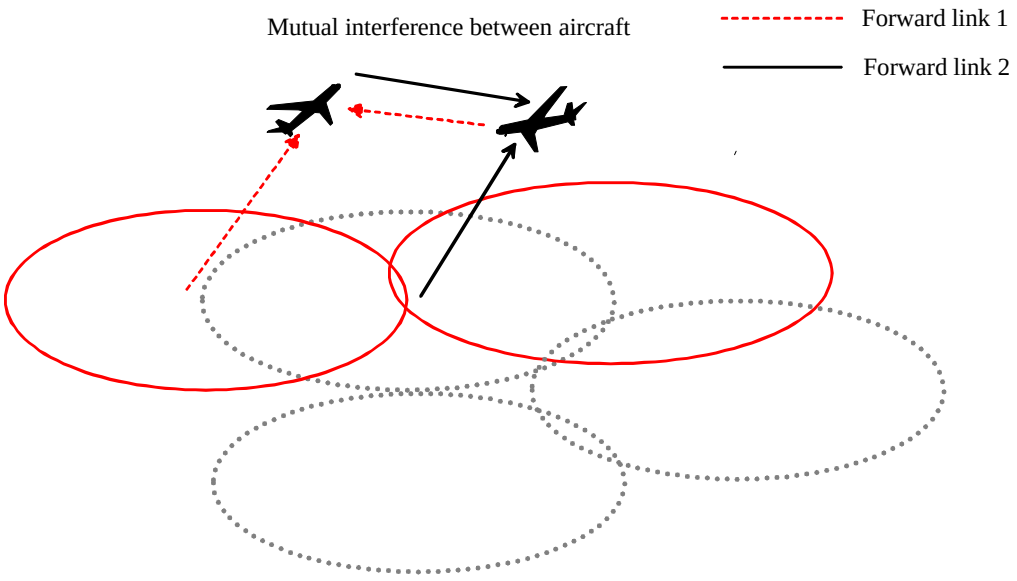

Figure 1: *Illustration of interference between aircraft that could occur with cross-duplexed frequency assignments.*

AirCell has described simulation results that it claims demonstrate that the aircraft-to-aircraft interference will have a minimal impact on performance, and the two "cross-

[1] This is to minimize effects of interference from the AN/SPS-49 air search shipboard radars used by the U.S. Navy, discussed in more detail later in this paper.

duplexed" systems can therefore coexist [2][3]. AirCell expressed the interference impact primarily as the average reduction in throughput in both absolute terms (kb/s) and as a percentage of the baseline throughput (i.e., with no cross-duplex interference).

As will be seen, the benign effects suggested by the AirCell analysis depend on the specific assumptions used by AirCell regarding the technology choice and the link budget factors. It is shown here that with different assumptions, the impact of the cross-duplex interference can be significant. This means that the reversed-duplexing approach will introduce significant, and at times debilitating, harmful interference to both ATG systems attempting to deploy a broadband communications service and will artificially limit the flexibility of operators in choosing their technology options and system design parameters.

The AirCell model assumed CDMA technology, with the reverse link traffic consisting of 9.6 kb/s speech circuits, and a pole capacity per sector of 40 such circuits. The highest load used by AirCell was 75%, corresponding to 30 speech circuits per sector on the reverse link. With a speech activity factor of 0.5, this represents an aggregate reverse link throughput of 144 kb/s. On the forward link (base to aircraft), AirCell assumed the 1xEV-DO air interface, which uses time division (to avoid in-cell interference that occurs with CDMA) and adaptive-rate modulation to deliver the maximum possible data rate to each mobile (aircraft) based on the signal-to-interference plus noise ratio (SINR, or E_c/N_t) at the mobile receiver. The peak rate available on the 1xEV-DO forward link is 2457.6 kb/s, and the average rate over a sector typically exceeds 1 Mb/s in a terrestrial environment. AirCell's results suggest that its average baseline forward link rate is also on the order of 1 Mb/s.

Thus, AirCell's analyses, and hence its conclusions, are predicated on the assumption of a highly unbalanced link,[2] using power-controlled code-division on the reverse link and rate-controlled time-division on the forward link. In addition, AirCell uses a "textbook" link budget, with no allowance for implementation losses or non-ideal propagation. Based on Airfone's operational experience, a reasonable margin for the aggregate effect of such factors is about 10 dB [4]. With the operating scenario assumed by AirCell, such additional penalties in the link budget have a two-fold effect. First, they weaken the desired signal received by the aircraft from its base station. Second, they cause the interfering aircraft to transmit more power on its reverse link to overcome the additional impairment. An additional base-to-aircraft loss of 10 dB therefore reduces the signal-to-interference ratio by 20 dB, at any given percentile point in its distribution (the significance of thermal noise, which is a constant, will also be increased).

Notwithstanding the exact values of assumed link budget parameters, the point is that the results are fairly sensitive to these parameters, which in itself makes duplex-inversion

[2] Although such asymmetry has been the traditional model for data transmission, AirCell was clearly modeling an aggregation of real-time speech circuits, at least on the reverse link. AirCell does not explain how this comports with the use of 1xEV-DO (which has a latency too high for speech) on the forward link.

questionable as a means for promoting efficient spectrum sharing. A further and perhaps larger issue is that of technology evolution. It is unreasonable to assume that EV-DO mobile radio technology will not continue to evolve and provide higher reverse link rates than can be supported by current technologies. Future air interfaces available to mobile radio carriers will undoubtedly support reverse-link data rates and spectral efficiencies much higher than those currently available. As is well-known, increasing spectral efficiency (bps/Hz) requires an increase in the SINR; see Figure 2. It can be seen that the textbook modulation formats shown (at a 10^{-4} bit error rate) roughly track a curve that is 6 dB worse than the Shannon bound. Also shown are points corresponding to the 11 rates available on the 1xEV-DO forward link [5].

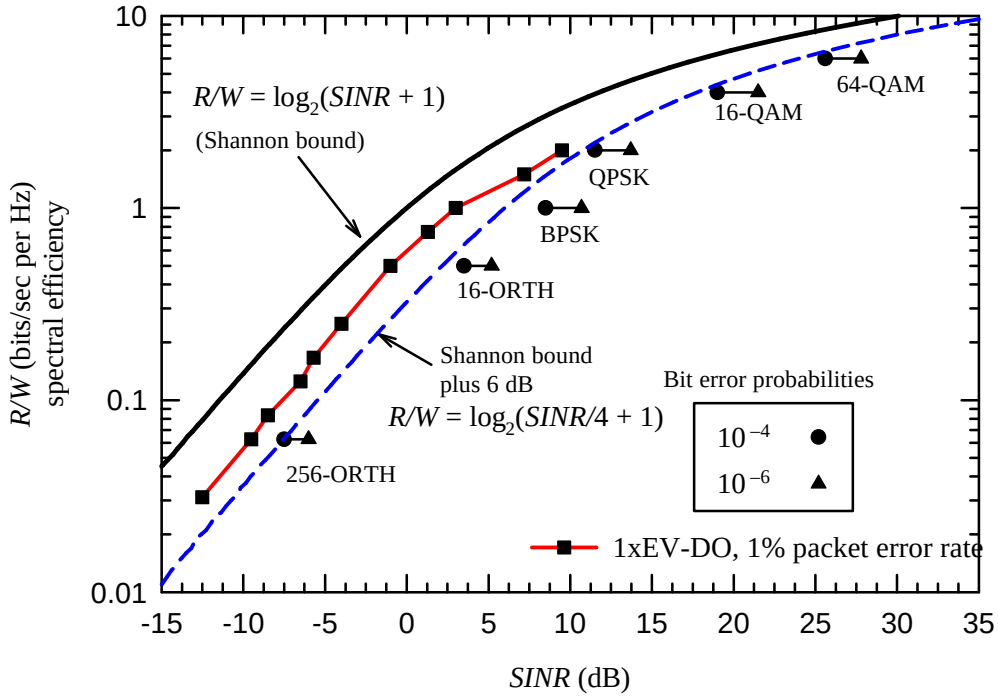

Figure 2: *Spectral efficiency vs. SINR*

Clearly, achieving higher spectral efficiency will require increasing the SINR at the base station receiver. This will in turn require higher reverse link transmit power, plus some means of reducing or eliminating same-cell interference on the reverse link. The latter could be achieved using a time-division approach (as is done on the 1xEV-DO forward link) or a frequency division approach, perhaps using some form of orthogonal frequency division multiplexing (OFDM).

For purposes of assessing the duplex-inversion scheme, the main point is that the reverse link transmit power is likely to be significantly higher than assumed by AirCell in its

simulations. AirCell assumed a maximum aircraft transmit power of 23 dBm (200 mW) to support ten 9.6-kb/s speech channels. This is the same as the maximum power level for a single terrestrial CDMA handset, supporting a single speech channel, and it is clear from AirCell's histograms that in some cases the 23-dBm maximum was inadequate.

However, even if the 23-dBm limit is removed, the basic model is completely inappropriate for representing future (i.e., "4G") technologies that may become available for ATG communications. AirCell's simulation, for each time sample, computes the power transmitted by each aircraft assuming ten active 9.6-kb/s speech connections per aircraft, a speech activity factor of 0.5, and perfect power control. The interference impact on the "other provider" aircraft is then determined by that transmit power, as well as the distance between the two aircraft and the position of the victim aircraft relative to its own base station. The reverse-link assumptions made by AirCell therefore drive the statistics of the power transmitted by the aircraft, which directly affects the calculated interference impact, however it may be expressed (loss in average forward link capacity, outage, etc.). Changing the assumed reverse-link paradigm to more closely match the forward link assumptions can therefore have a significant effect on the results.

This paper is organized as follows. Section 2 briefly summarizes the AirCell simulation framework and its limitations. Section 3 describes a "square grid" simulation that was developed to explore aircraft-to-aircraft interference scenarios similar to AirCell's, and to test the sensitivity of the results and conclusions to changes in the parameters. Results are provided for parameters similar to those used by AirCell and compared to AirCell's results, and then results for different parameters are provided. Sensitivities of the results to various simplifications in the simulation are also investigated. Section 4 develops a more extensive simulation that accounts for real world factors such as non-uniform air traffic distribution, sectorized base station antenna patterns, sectorized aircraft antennas with best-beam selection and actual existing base station locations across the continental U. S. Section 5 discusses the potential for interference from Naval air search radars to reverse-duplexed aircraft high-band receivers, and Section 6 addresses adaptive antenna issues for coexistence of multiple systems in the same ATG bands. Annex A derives the simple expression used here for the radio horizon and Annex B derives the CDMA reverse link capacity and load factor. Annex C develops a simplified model for the effect of the cross-duplex interference in terms of the EIRP of the base station, the maximum EIRP of the power-controlled aircraft transmitter, and the number of interfering aircraft in the same cell as the victim aircraft. The results are shown to agree very closely with those of the full square-grid simulation. Using this model, the outage probabilities for aircraft in the outer 50%, 25%, and 10% of the cell area are shown.

2. The AirCell Simulation Framework

2.1. Overview of the AirCell Simulation

Figure 3 shows the geometry used by AirCell in its simulations, which investigated two different scenarios. For the "cross-country" scenario, $D = 200$ mi and for the "airport scenario" $D = 25$ mi. The frequency duplexing of network 2 is reversed compared to that of network 1.

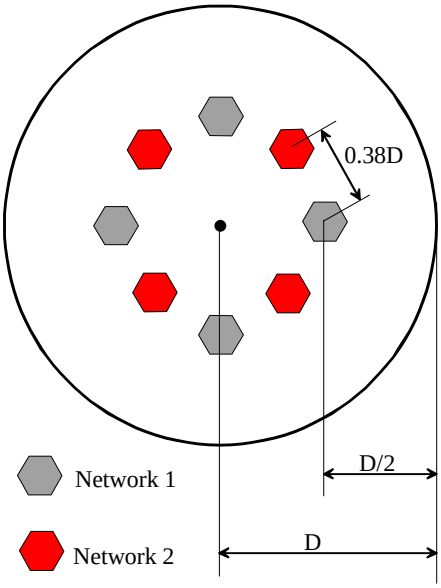

Figure 3: *The AirCell simulation model geometry.*

AirCell simulates aircraft-to-aircraft interference based on this geometry. Base-to-base interference is ignored on the assumption that base stations of different systems will be separated by a distance exceeding their mutual radio horizon. However, this clearly is not true for the AirCell "airport scenario". The radio horizon between two points elevated h_1 and h_2 feet above the surface of the Earth is (see Annex A)

$$d_{rh} = \sqrt{2}\left(\sqrt{h_1} + \sqrt{h_2}\right) \text{ miles} \quad (1)$$

For $D = 25$ mi base stations of the two different networks can be within 9.5 miles of each other. Antenna heights range from 40 to 240 feet above ground, corresponding to tower-to-tower radio horizons ranging from 17.9 to 43.8 miles, so in AirCell's airport scenario, each base station will be within the radio horizon of at least two interfering (reverse-duplexed) base stations. It will also be a concern in a real-world deployment

situation as antennas will tend to be higher in built-up areas near major airports. Therefore, in a normal major airport environment, base-to-base interference is extremely likely. Such base-to-base interference will completely eliminate any communications between the base and aircraft and cannot be ignored for general ATG system operations.

For the cross-country scenario, AirCell assumes omnidirectional antennas at the base stations. Each aircraft is assumed to carry ten active 9.6 kb/s speech circuits on the reverse link, and the aircraft transmit power is calculated based on a typical CDMA power-controlled reverse link model. That is, the transmit power needed to meet the required E_b/N_t at the base station receiver will therefore depend on the path loss between the aircraft and the base station as well as the total power received by the base station. However, there is a minor error in AirCell's mathematical model for the reverse link (see Annex B). In addition, AirCell aggregates the ten speech channels into a single 76 kb/s stream per aircraft. As a result, it is unclear exactly how the required power at the base station receiver was computed.

In any case, AirCell computes the power transmitted by the aircraft based on ten 9.6 kb/s speech circuits, each with a speech activity factor of 0.5, so the average reverse link data rate per aircraft is 48 kb/s.[3] AirCell calculates that the pole capacity of a cell corresponds to about 4 such aircraft, and 3 different load scenarios are explored using 1, 2, and 3 aircraft per cell, corresponding to 25%, 50% and 75% load, respectively. Based on the power levels transmitted by the aircraft, the distances to the "other system" aircraft, and the desired signal power levels received by all the aircraft, the signal to interference plus noise ratio (SINR) is computed at each aircraft receiver, and used to determine the maximum supportable data rate based on the 1xEV-DO forward link rate table. Statistics on SINR and data rate are collected and output is expressed in terms of the reduction in average data rate, and the distribution of the SINR reduction due to the cross-duplex interference. Results are provided for both 100% and 40% spectral overlap.

Similar computations are performed for the airport scenario, except that as indicated above, the cells are much smaller. Also, it is assumed that there are 3 sectors per cell so that each 25% of loading corresponds to 3 aircraft per cell rather than 1. In all cases, AirCell shows the reduction in total average forward link throughput to be small.

2.2. Comments on the AirCell Model

2.2.1. Minor Observations

- AirCell assumed a 4-cell square cell layout geometry for each system, with system 2 rotated 45° with respect to system 1. If this layout is extended to more cells, it appears as in Figure 4, which results in some of the system 1 and system 2 base stations being very near each other. An alternative would be to use a half-cell offset

[3] In its simulation, AirCell hard-limits the maximum total transmit power per aircraft to 23 dBm (200 mW).

in each dimension as shown in Figure 5, which can be uniformly replicated over a plane.

- AirCell's reverse link pole point formula has a minor error as discussed in Annex B.
- It is unclear what service is being modeled, since speech was used on the reverse link but high speed data with 1xEV-DO (which does not support speech) was used on the forward link. From a mechanical perspective, the reverse link speech circuits simply serve to provide a means of computing the aircraft transmit power.
- It is unclear how AirCell accounted for the interference to the aircraft from other base stations of the same system. Such interference does not seem to be included in the "worst case" interference calculations in section 5 of the AirCell paper.

2.2.2. Major Deficiencies

- The link budget assumptions were idealized, assuming perfect propagation with no reflections, no system implementation losses, and perfect power control.
- The simulations considered a very limited (and somewhat artificial) case consisting of a low-rate, low-power speech-only reverse link and a high-rate, high-power, data-only forward link. The average reverse link rate is 48 kb/s per aircraft under AirCell's model, or a total of 144 kb/s per cell (or sector) for the 75% loading case. In contrast, the average forward link rate seems to be on the order of more than 1 Mb/s.
- No sensitivity analyses were performed to determine the interference impact under other sets of conditions.

As will be seen in the following sections, including the effects of imperfect conditions, and accounting for higher-speed reverse link transmissions, will dramatically change the conclusions about the impact of the cross-duplex interference.

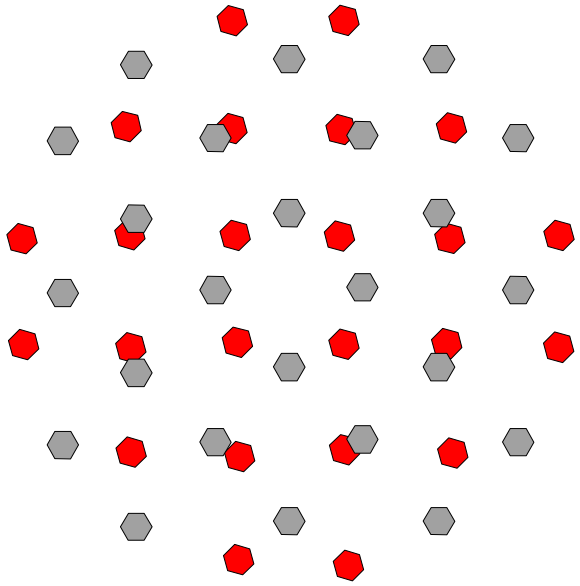

Figure 4: *Replication of the AirCell layout*

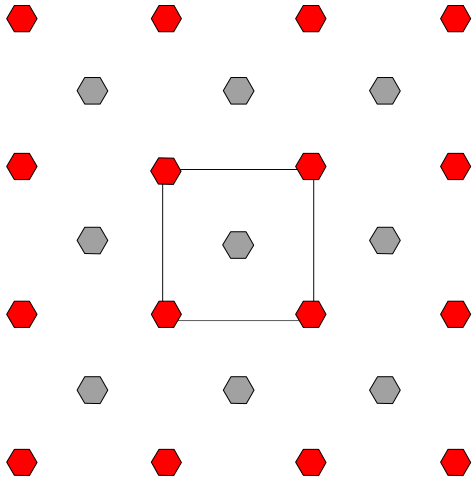

Figure 5: *Square cell layout with other-system offset*

3. Square-Grid Simulation

3.1. General Description

To explore the sensitivity of the cross-duplex interference impact to various assumptions, a simulation similar to AirCell's was created based on a square grid layout, and its results were compared to those from the AirCell simulations. As this section discusses, the square-grid simulation accurately replicates AirCell's results when assumptions similar to AirCell's are used. This section describes the development of the square-grid simulation and demonstrates that it is consistent with the model AirCell used in its analysis.

A Monte Carlo approach was used. For each sample, the victim aircraft is randomly located within its cell (lateral position and altitude) and the received desired signal power is calculated. This can be done in one of two ways: (1) using the nearest base station; or (2) using the strongest forward link signal. These two may be different if the aircraft is at a high elevation angle with respect to the base station. Figure 6 shows the pattern assumed by AirCell in its simulation. In the simulation discussed here, it was assumed that the gain is 9 dBi for elevation angles up to 15°, and –11 dBi for greater elevation angles. Thus, depending on the size of the cell and the aircraft elevation, a stronger signal might be available from an adjacent cell.

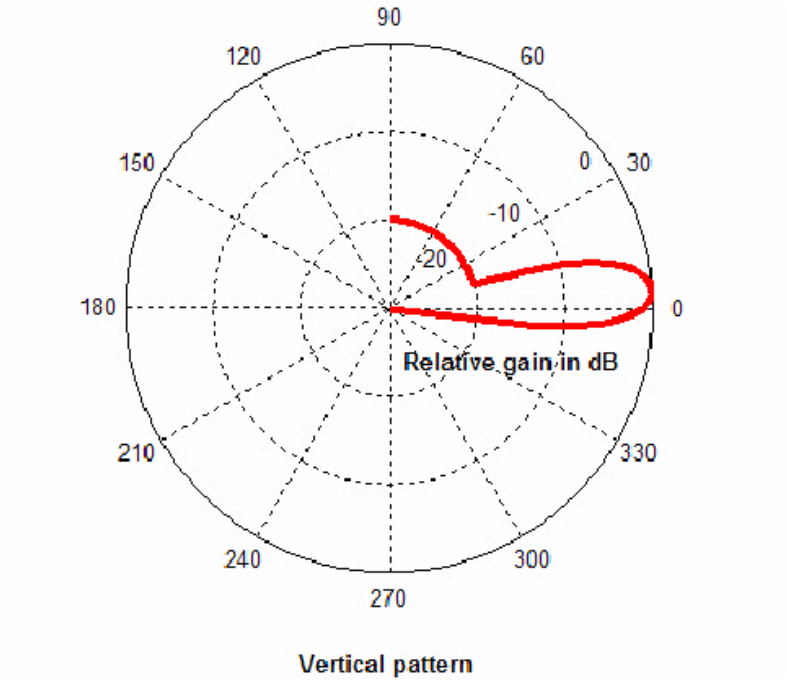

Figure 6: *AirCell vertical gain antenna pattern for cross-country scenario (reproduced from Figure 14 of the AirCell paper). The maximum gain is 9 dBi.*

After computing the received desired signal power, the algorithm calculates the total interference from the aircraft of the second (reverse-duplexed) network, which also uses a square cell site layout. There are two options for positioning the cell site grid of the second network relative to that of the first: (1) random offset with a different offset for each sample; and (2) half-cell offset (in both dimensions), per Figure 5.

For each cell of the second network, the following calculations are performed for each aircraft in the cell (the number of aircraft per cell depends on the selected load):

- The aircraft position in the cell (*x*, *y*, and altitude) is randomly generated.
- If the separation between the aircraft and the victim (system 1) aircraft exceeds the radio horizon, the aircraft is ignored.
- The path loss from the aircraft to the strongest base station is computed, including effects of distance, antenna gain, and system losses (parameters that can be set).
- Each of ten speech channels is randomly assigned an active or idle state (each with 50% probability) to reflect speech activity. If a channel is idle, it contributes 1/8 the transmit power of an active channel.
- The transmit power of the aircraft is computed based on the path loss, the number of active speech channels, and the required received signal power at the base station.
- Based on this transmit power and the distance to the victim aircraft, the interference received by the victim aircraft is computed and added to the running total interference.

The interference from the other-system aircraft is added to the interference from the same-system other-cell base stations, the total SINR is computed, and the corresponding maximum achievable 1xEV-DO is determined (a look-up). If the SINR is below –12.5 dB, even the lowest 1xEV-DO rate cannot be supported, and an outage is recorded.

When complete, the simulation can report on statistics such as the average rate, the average rate compared to the stand-alone system case, the outage probability, various distributions (e.g., the data rates, transmit power levels), etc.

3.2. Link Budgets

The key components of the simulation are the link budget factors for the forward and reverse links.

The power received at the aircraft is

$$P_{RX,AC} = P_{B,TX} + G_B(f_{AC}) - L_{cabl} - L_{dipl} - L_{fs}(d_{B-AC}) - M_{sys} \text{ dBm} \qquad (2)$$

where $P_{B,TX}$ is the transmit power at the base station into the antenna terminals, f_{AC} is the elevation angle of the aircraft relative to the base station, $G_B(f_{AC})$ is the elevation gain of the base station antenna, L_{cabl} and L_{dipl} are cable and diplexer losses, respectively, d_{B-AC} is the distance between the base station and the aircraft, and M_{sys} is a system performance margin that accounts for non-idealities in propagation and implementation, including the effects of multipath and variations in antenna gain due to tolerance in the tilt and horizontal orientation. Based on Airfone's operational experience, an appropriate value for M_{sys} is about 10 dB [4]. $L_{fs}(d)$ is the free space path loss for a distance d, which at a frequency of 870 MHz with *d* in miles is:

$$L_{fs}(d) = 95.3 + 20 \log d \quad \text{dB}. \tag{3}$$

Figure 7 shows $P_{RX,AC}$ vs. d_{B-AC} for the parameters listed in the caption.

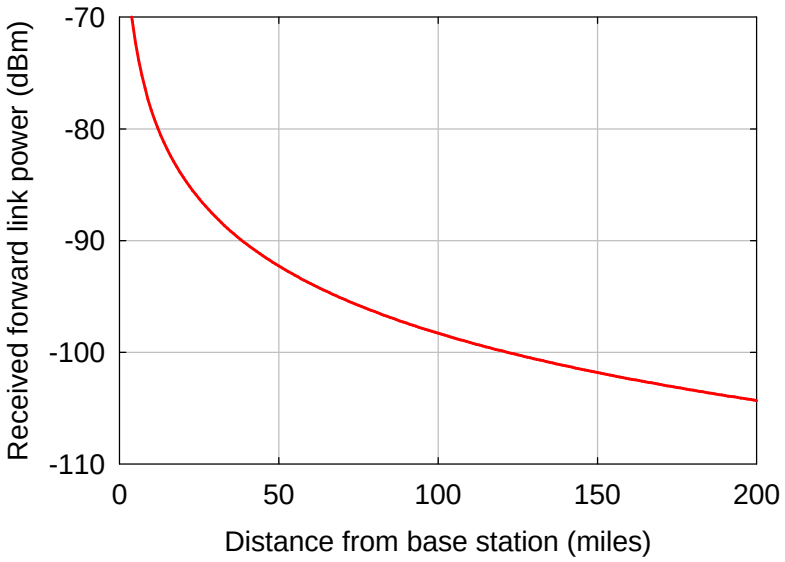

Figure 7: *Received forward link power vs. distance for* $P_{BTX} = 43\,\text{dBm}$, $L_{cabl} = 3\,\text{dB}$, $L_{dipl} = 2\,\text{dB}$, $G_B = 9\,\text{dB}$, and $M_{sys} = 10\,\text{dB}$.

Assuming perfect power control, the EIRP that the aircraft must transmit per voice circuit is

$$EIRP_{AC} = -113 + F_{noise} + F_{load} - M_J + F_{ckts} - G_B(f_{AC}) + L_{cabl} + L_{dipl} + L_{fs}(d_{AC-B}) + M_{sys} \text{ dBm} \quad (4)$$

where F_{noise} is the noise figure, F_{load} is the CDMA reverse link load factor (from the load curve – see Annex B), F_{ckts} accounts for the number of voice circuits that are active, M_J is the CDMA reverse link jamming margin, and d_{AC-B} is the distance from the aircraft to the receiving base station.

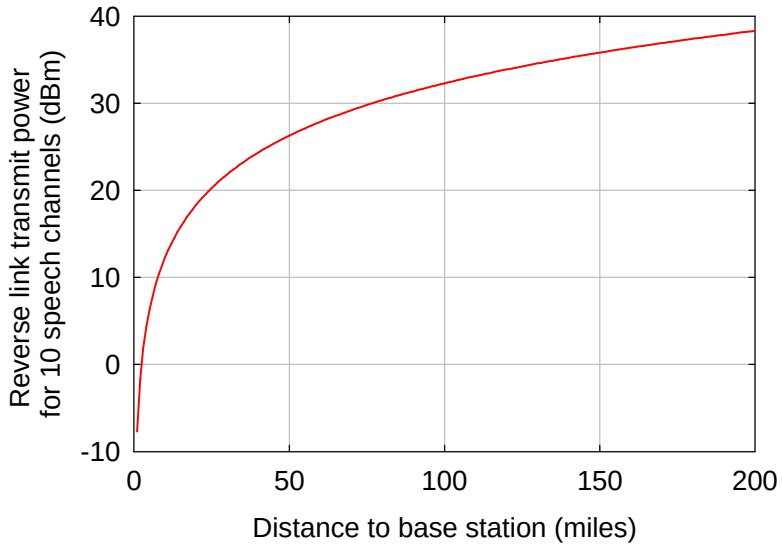

Figure 8: *Reverse link transmit power vs. distance* for $F_{noise} = 5\,\text{dB}$, $F_{load} = 6\,\text{dB}$, $L_{cabl} = 3\,\text{dB}$, $L_{dipl} = 2\,\text{dB}$, $G_B = 9\,\text{dB}$, $M_J = 17\,\text{dB}$, $M_{sys} = 10\,\text{dB}$, and $F_{ckts} = 10\,\text{dB}$.

Finally, the interference power received by the victim aircraft is

$$I_{AC} = EIRP_{AC} - L_{FS}(d_{AC-AC}) \text{ dBm} \quad (5)$$

where d_{AC-AC} is the distance between the aircraft in miles. Note that these relationships imply a gain of 0 dBi for the aircraft antenna and a lossless aircraft receive chain. Also, they do not account for the effects of imperfect power control.

For all of the results reported here, $L_{cabl} = 3\,\text{dB}$, $F_{noise} = 5\,\text{dB}$, $M_J = 17\,\text{dB}$ (assuming a 9.6 kb/s data rate and a 4-dB E_b/N_t requirement), and $G_B = 9\,\text{dB}$ (unless the elevation angle exceeds 15°, in which case the gain is reduced by 20 dB). Also, the minimum

horizontal separation between the interfering and interfered aircraft was 5 miles and the aircraft antenna was assumed to be isotropic as was also assumed by AirCell – see p. 17 of the AirCell paper [3].

3.3. Outer-Cell Forward Link Interference

With the square cell geometry, an aircraft at the cell corner receives equal power from the serving cell and each of 3 interfering cells as shown in Figure 9. In Figure 10, the SINR is shown as a function of distance from the base station (relative to the cell dimension *D*) for several different azimuth angles q. The base station antenna height was assumed to be 100 feet and the aircraft was assumed to be flying at 30,000 feet. Discontinuities correspond to points at which an interfering base station was just at the radio horizon. The 20-dB drop at small *d* is due to the assumed antenna pattern, which drops from +9 dBi to –11 dBi for elevation angles exceeding 15°. As can be seen, the SINR is not very sensitive to azimuth angle.

The approximation assumes that the total interference from all outer-cell base stations is constant over the cell and that the desired signal varies according to free space path loss. As can be seen, agreement is reasonably good for the 30,000-foot aircraft altitude assumed. Figure 11 shows the SINR vs. d/D for an aircraft altitude of 18,000 feet, which is the minimum altitude considered in the cross-country scenario. The impact of representing the outer cell interference as a constant was explored as discussed below.

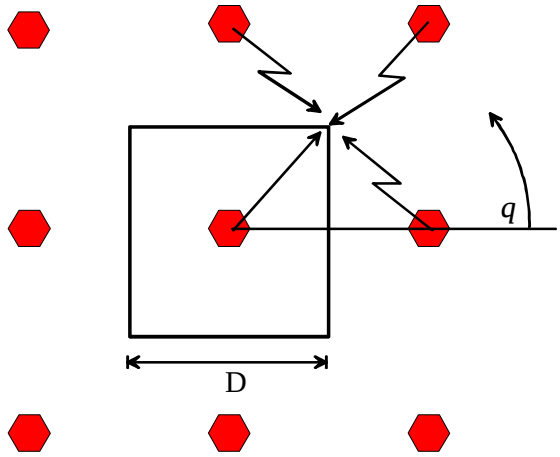

Figure 9: *Outer cell forward link interference at cell corner.*

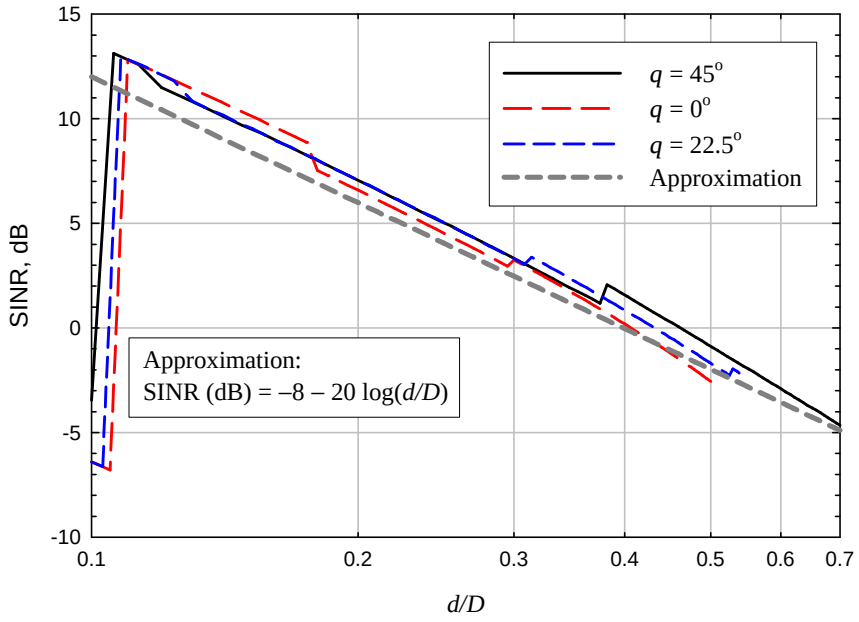

Figure 10: *SINR with outer cell forward link interference vs. relative location in cell for* $D = 200$ *miles and an aircraft altitude of 30,000 ft.*

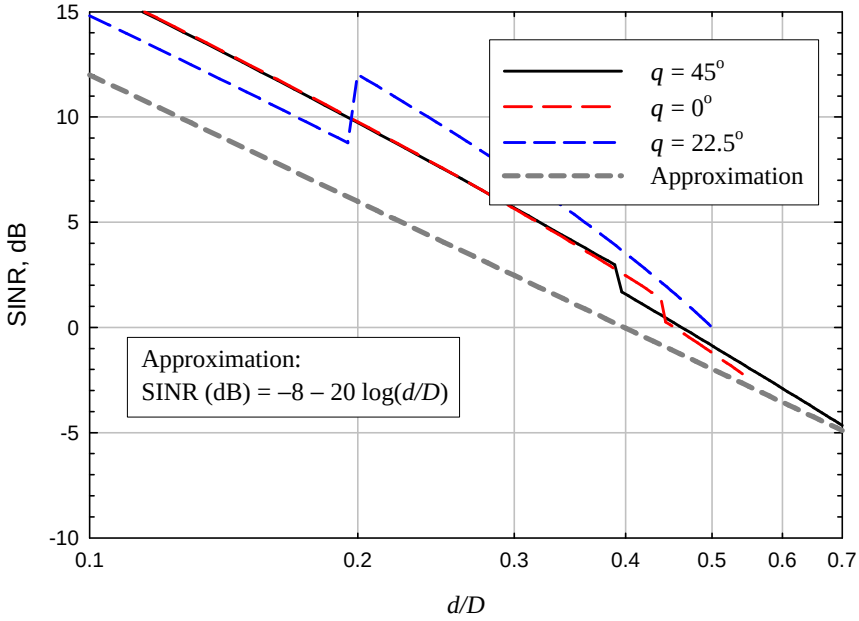

Figure 11: *SINR with outer cell forward link interference vs. relative location in cell for* $D = 200$ *miles and an aircraft altitude of 18,000 ft.*

3.4. Simulation Variations and Results

To determine which factors are most important in determining the results, a number of variations on the simulation were explored. These include:

- Varying aircraft altitude randomly between 18,000 and 40,000 feet vs. using a single 35,000-foot altitude for all aircraft.
- Computing the actual same-system forward link other-cell interference (OCI) vs. approximating the OCI as a constant as discussed above.
- Computing the received forward link power to the victim aircraft based on the nearest base station vs. the strongest base station.
- Using a fixed offset between the base station grids of the two systems vs. a random offset (randomly generated for each simulation sample).

The cases tested suggest that, at least within the parameter space that was explored, none of these factors make a significant difference in the results. In fact, as shown in Annex C, a relatively simple model can be used to obtain results that closely match those of the more complex and detailed simulation.

The basic simulation geometry is as shown in Figure 5, where the victim aircraft is randomly-located within the square centered on the base station in the center of the grid. A single tier of same-system base stations surround the center cell, and are used to compute the other-cell forward link interference as well as to search for a stronger forward link transmission if the aircraft elevation angle is above 15°. There are 16 other-system base stations surrounding the center base station. This number can be increased or reduced, and the offset can be made fixed as shown at $D/2$ in each dimension, or generated randomly for each sample.

For comparison with the AirCell results, a modified geometry was shown in Figure 12, which is a subset of the full geometry with only four cells in each system. Table 1 shows a comparison with the AirCell results for the cross country scenario with 100% spectrum overlap. One million simulation samples were used for each value of load.

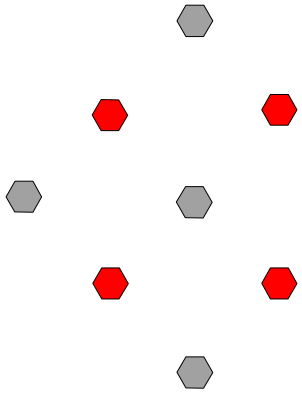

Figure 12: *Simulation geometry for comparison with AirCell results.*

The cable loss was assumed to be 3 dB in all cases, consistent with AirCell's assumption (see AirCell table 2, p. 20). It was found that if, in addition, a 2-dB diplexer loss was added, the results were very close to those reported by AirCell. If no diplexer loss is included, the effect of the interference is less than reported by AirCell, as shown in Table 1. The baseline average forward link rate, with no interference, was about 1Mb/s, which is close to the AirCell result, which can be inferred by comparing the absolute and percentage losses in columns 2 and 3 of Table 1 (e.g., 2 kb/s ÷ 0.0019 = 1052 kb/s).

Table 2 shows the comparison if the full geometry is used for the square grid simulation, per Figure 5. The baseline average forward link rate for the square grid simulation is about 670 kb/s. This is lower than the rate for the reduced geometry due to the additional other-cell forward link interference (the cell is surrounded on all sides by same-system base stations). The SINR is therefore generally lower, and the average supportable forward link rate is therefore lower. Overall, the square grid simulation shows less interference impact than the AirCell results for comparable parameters. If a 2-dB diplexer loss is added to the square grid simulation, the results appear comparable (this is a realistic value for the loss associated with the diplexer and it is unclear why AirCell neglected it).

Table 1: *Comparison of the square-grid simulation (reduced geometry) and AirCell results for the cross-country case, 100% spectrum overlap (see AirCell Figure 45, page 69).*

loading	AirCell Fig. 45		2 dB diplexer loss		0 dB diplexer loss	
	kb/s	%	kb/s	%	kb/s	%
25%	2.03	0.19	1.58	0.15	0.61	0.058
50%	6.25	0.55	6.40	0.61	0.69	0.065
75%	19.84	1.78	19.9	1.89	6.65	0.63

Table 2: *Comparison of AirCell results with full-geometry square-grid results.*

loading	AirCell Fig. 45		0 dB diplexer loss – full geometry	
	kb/s	%	kb/s	%
25%	2.03	0.19	0.13	0.019
50%	6.25	0.55	1.08	0.16
75%	19.84	1.78	4.06	0.60

Since AirCell provides histograms of the Aircraft transmit power, it is also possible to compare the two simulations on that basis, as shown in Figure 13 to Figure 18 for 25%, 50%, and 75% loading for the cross-country case. The percentage of spectrum overlap does not affect the power transmitted by the aircraft. The histograms have somewhat different shapes as would be expected, since the shape of the histogram depends on the shape of the cell boundary. The square grid simulation reported here uses square cell boundaries, while the AirCell simulation apparently uses 90° "pie slice" boundaries, since the outer bound of the simulation area is the circle of radius *D*. Also, it is not completely clear how AirCell related the load percentage to the required received signal power at the base station. However, the aircraft transmit power distributions seem to be in reasonable general agreement. Note that the histograms shown here for the square grid simulation do not include the 2 dB diplexer loss. Also, the square grid simulation places no limit on the total aircraft EIRP, whereas the AirCell simulation limits the aircraft transmit power to 23 dBm. The effect of this limit can be seen in the histogram of Figure 18, which show a disproportionately high probability corresponding to 23 dBm, reflecting the fact that in some cases, more transmit power would have been used had it been available.

Overall, these comparisons of the two simulations suggest that when similar parameters are used, the results agree reasonably well. Therefore, the square-grid simulation model developed for this analysis can be used with modified parameters that are associated with real-world operations of an ATG system, rather than the textbook assumptions used by AirCell in its modeling.

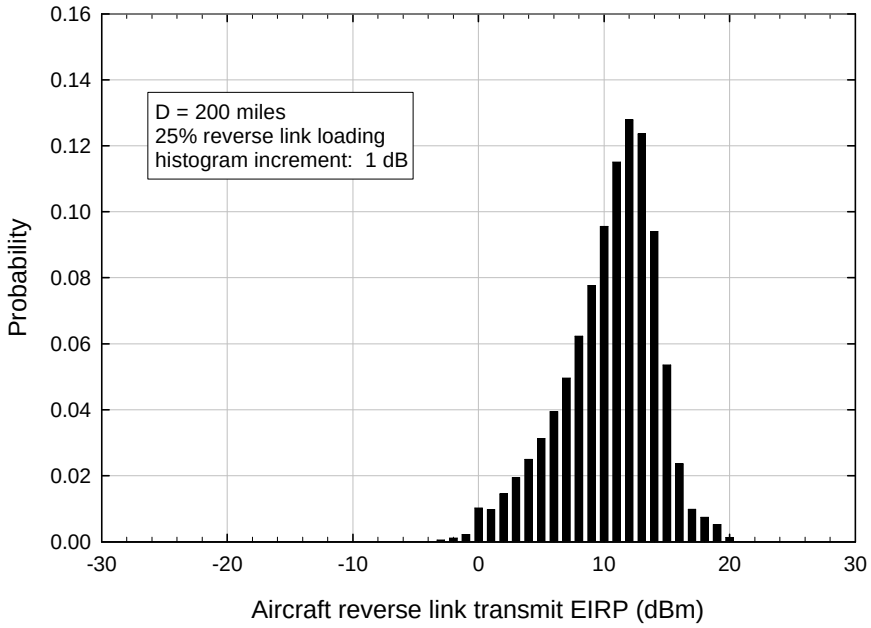

Figure 13: *Aircraft EIRP histogram from square grid simulation – 25% loading.*

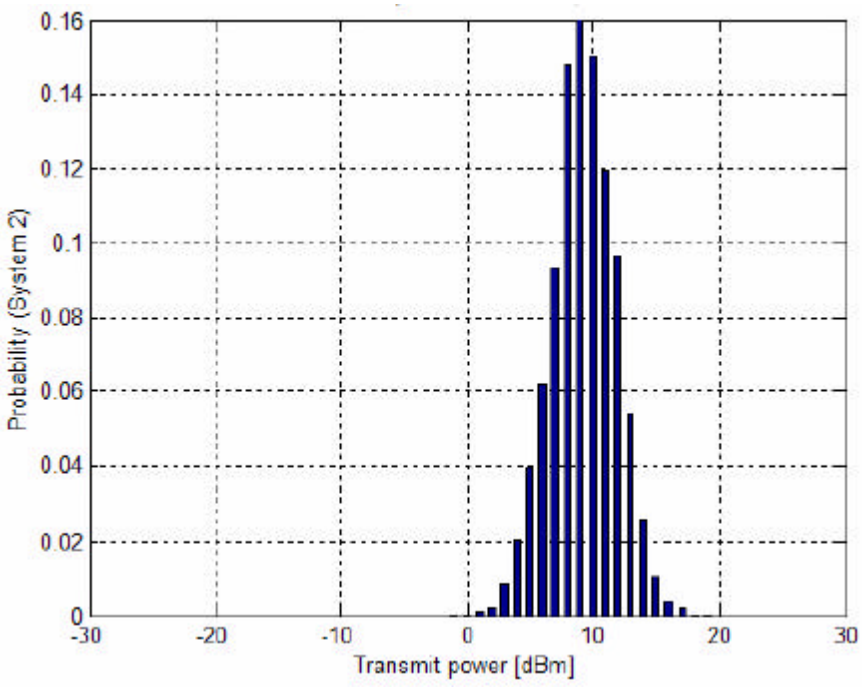

Figure 14: *Aircraft transmit power histogram for 25% loading (AirCell Figure 38, p. 62).*

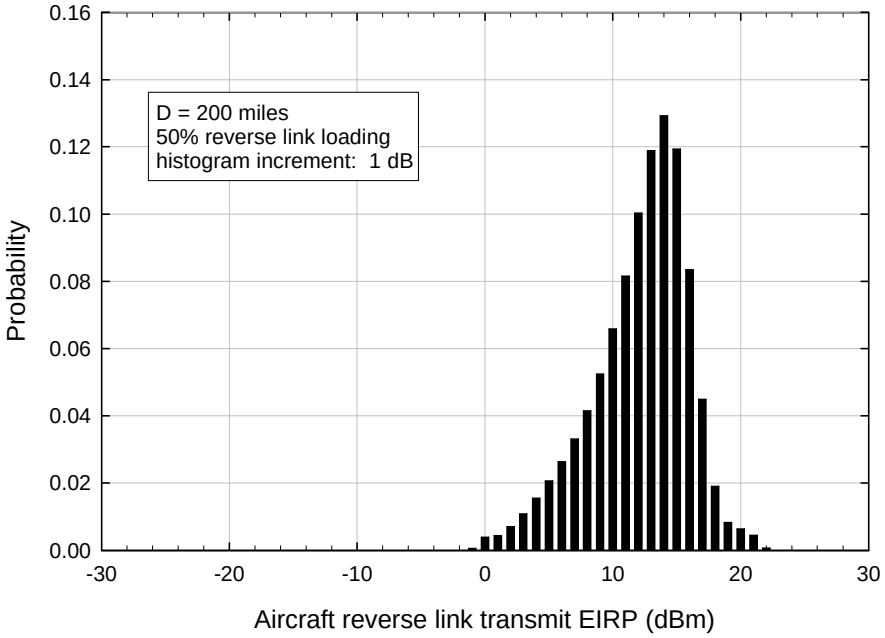

Figure 15: *Aircraft EIRP histogram from square grid simulation – 50% loading.*

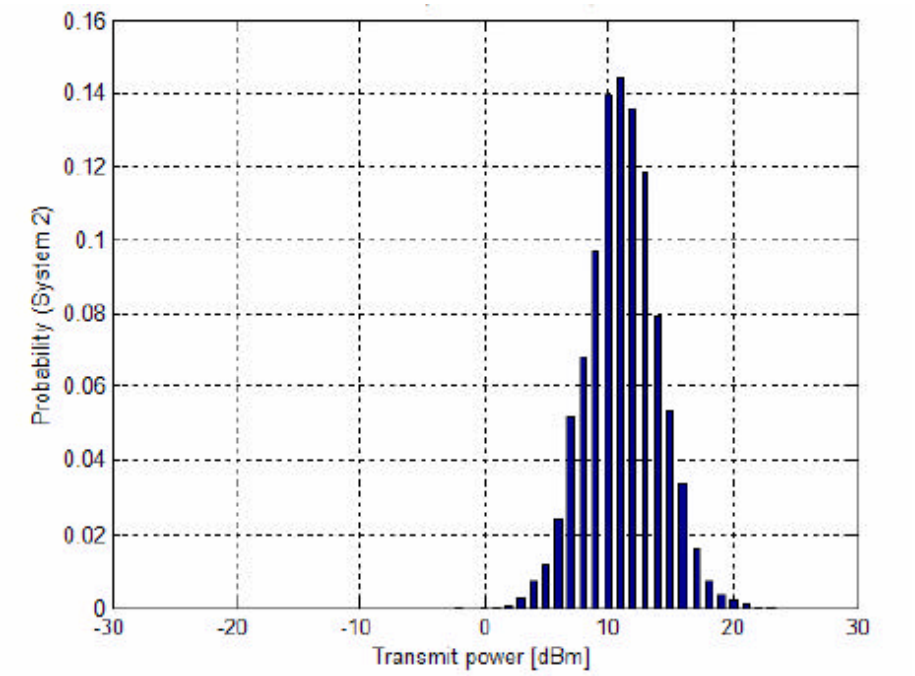

Figure 16: *Aircraft transmit power histogram for 50% loading (AirCell Figure 41, p. 65).*

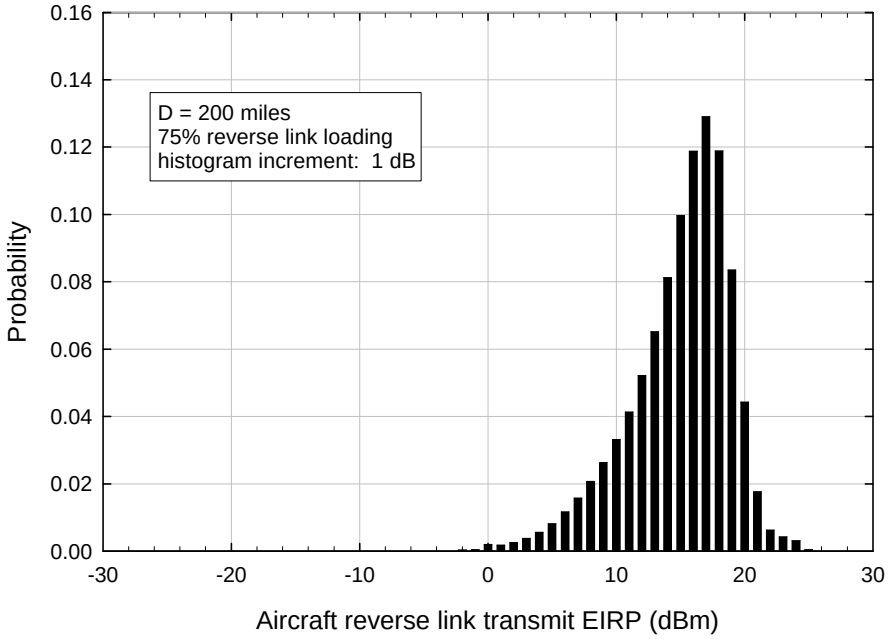

Figure 17: *Aircraft EIRP histogram from square grid simulation – 75% loading.*

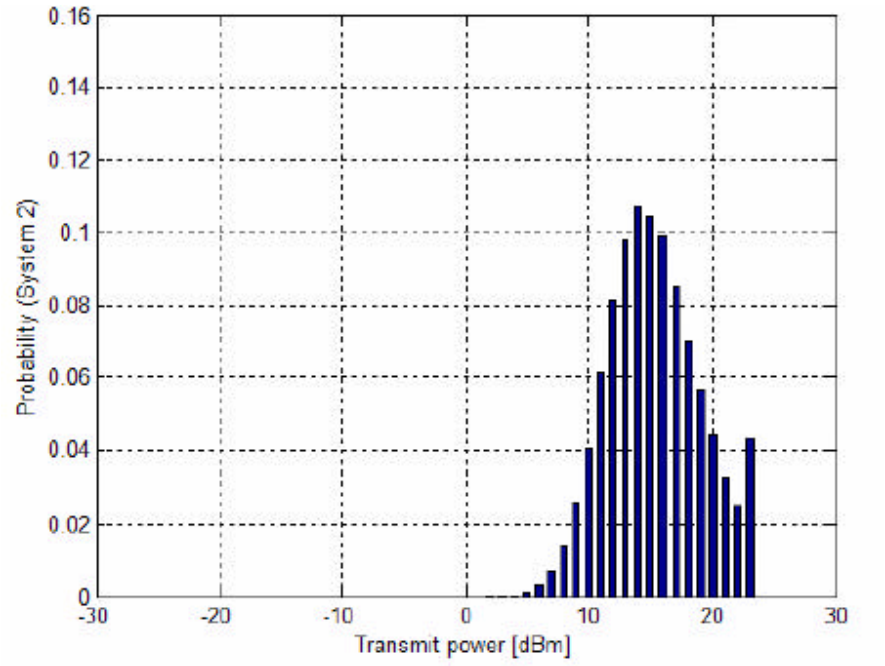

Figure 18: *Aircraft transmit power histogram for 75% loading (AirCell Figure 44, p. 68).*

3.5. Average Rate, Outage Probability, and Sensitivity to Simulation Mechanics

Figure 19 shows the average forward link capacity per cell and the outage probability vs. the number of interfering aircraft per victim cell. It was assumed that $M_{sys} = 10\,\text{dB}$, and $F_{load} = 6\,\text{dB}$ (the noise plus interference is 6 dB above thermal noise) for all cases, and perfect reverse link power control was assumed. Aircraft altitude was assumed randomly distributed between 18,000 and 40,000 feet and the base station tower elevation was assumed to be 100 feet. The minimum lateral separation between interfering aircraft was 5 miles. An outage corresponds to an SINR less than –12.5 dB, so that even the lowest 1xEV-DO rate cannot be supported. The simulation geometry was as shown in Figure 5, and 100% spectral overlap was assumed.

To explore the sensitivity of the results to the details of the simulation, changes were made in the simulation while retaining the same parameters used to generate the results of Figure 19. The changes are cumulative; each case retains the changes made in the previous case and adds one additional change:

- Figure 20 uses a random grid offset between the two systems rather than a fixed half-cell offset.
- Figure 21 uses a fixed aircraft altitude (35,000 feet) rather than a variable altitude.
- Figure 22 approximates the outer cell same system forward link interference as a constant rather than calculating it for each case.
- Figure 23 uses the nearest base station for the desired signal instead of searching for the strongest.

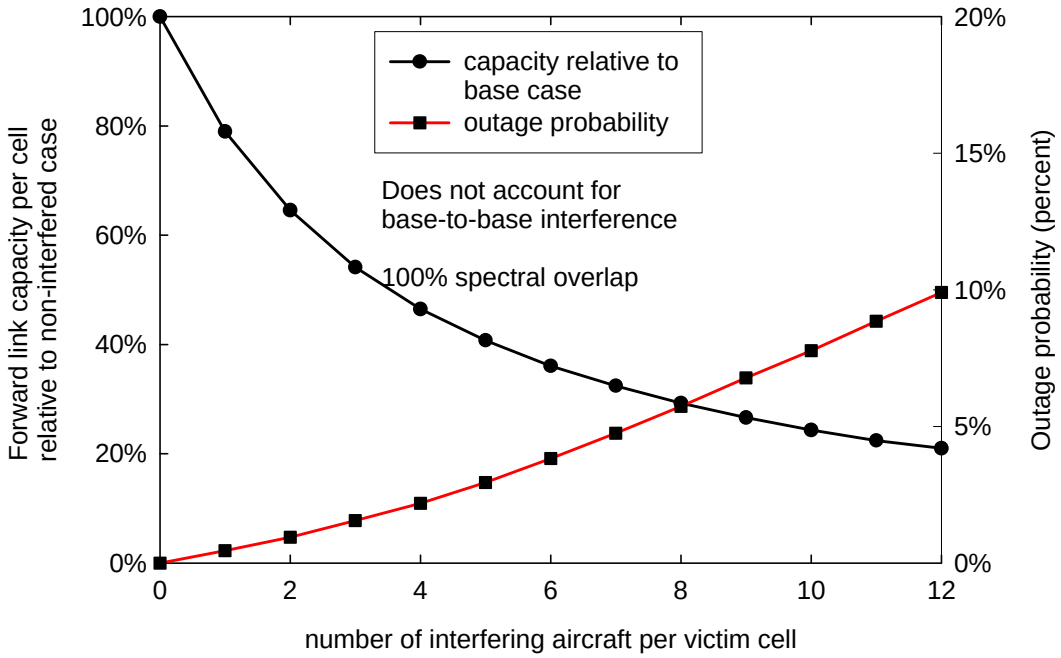

Figure 19: *Simulation results with $M_{sys} = 10\ dB$, half-cell offset between the grids of system 1 and system 2.*

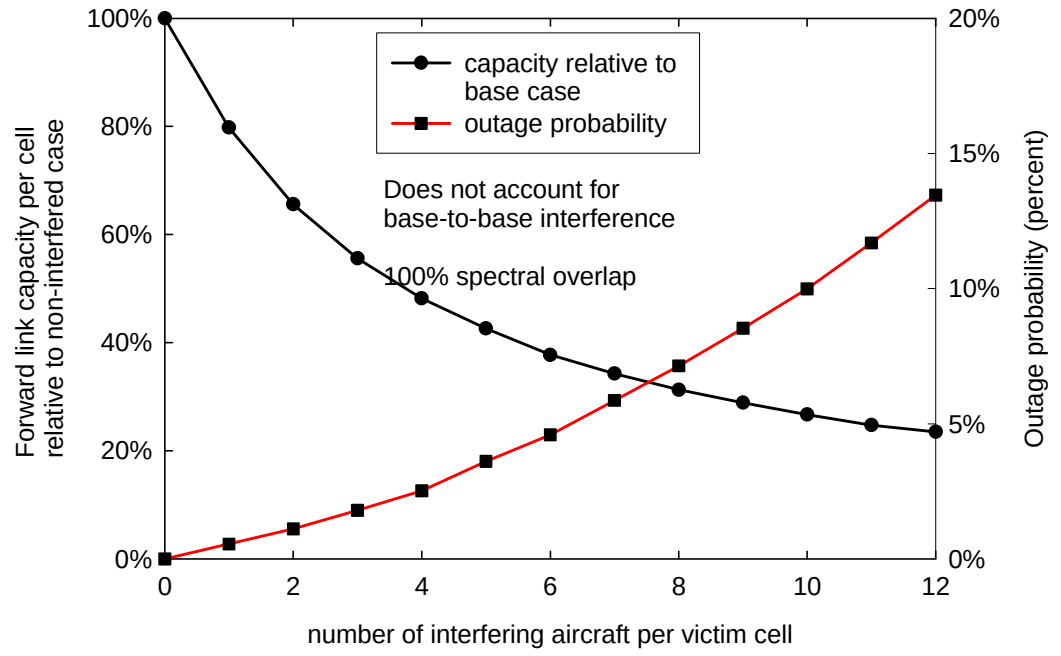

Figure 20: *Same as Figure 19 except with random offsets between the grids of systems 1 and 2.*

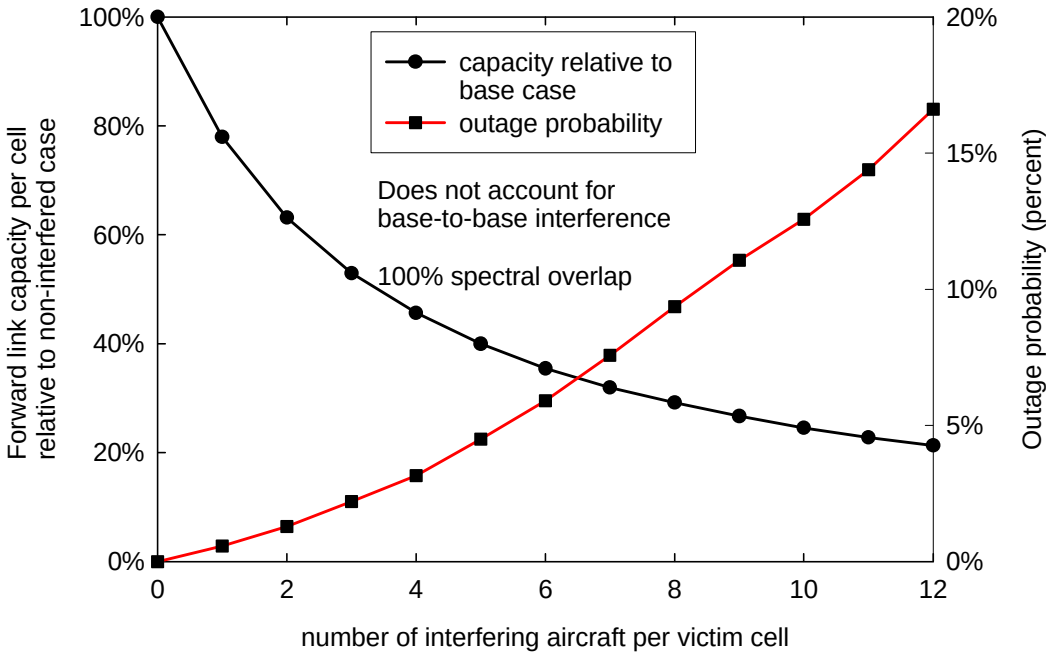

Figure 21: *Same as Figure 20 except aircraft altitude is fixed at 35,000 feet.*

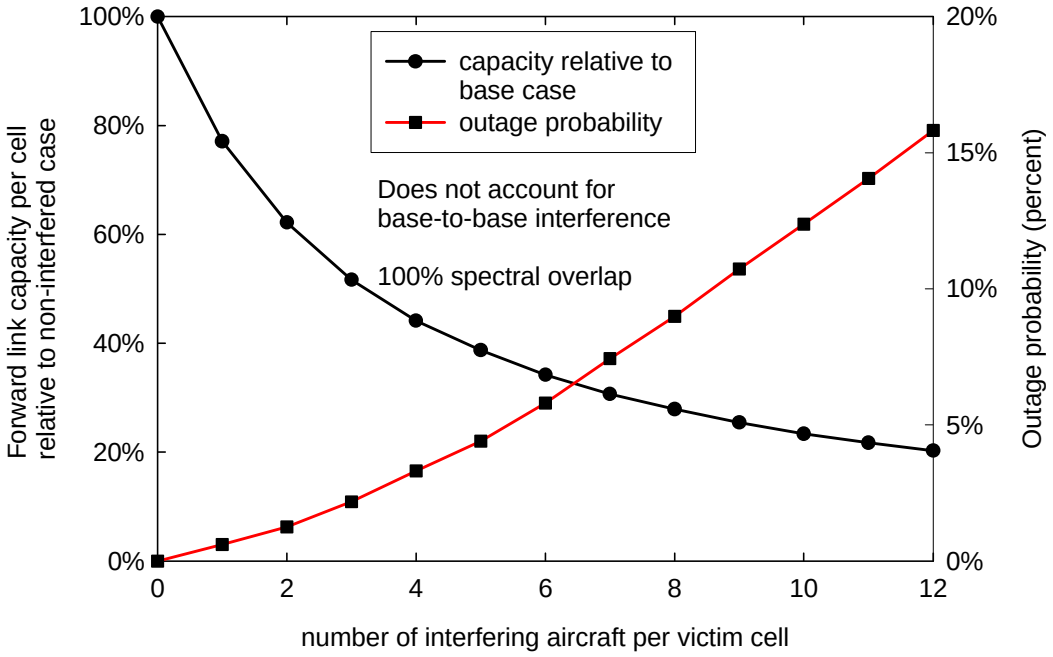

Figure 22: *Same as Figure 21 except that outer-cell forward link interference is approximated as a constant.*

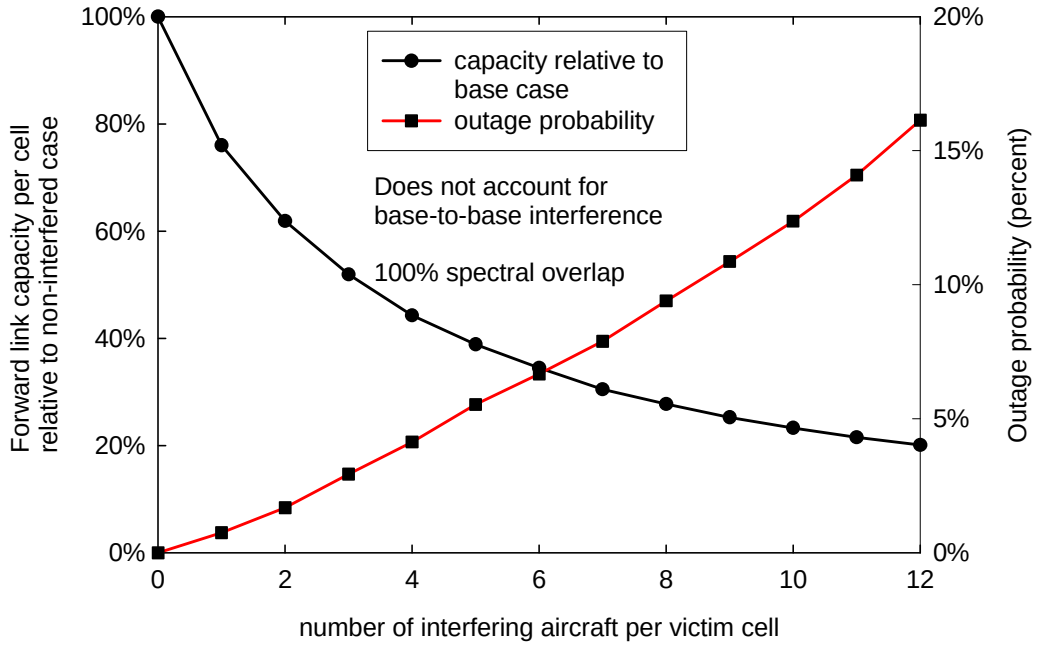

Figure 23: *Same as Figure 22 except that nearest base station is used for desired signal (regardless of antenna gain).*

As can be seen, the factor which seems to make the most difference is the randomization of the offset between the cell grids of the two systems. The net effect of all the approximations is to increase the outage probability somewhat, but the impact on the average forward link rate is fairly small.

Figure 24 shows the aircraft EIRP histogram for these cases ($M_{sys} = 10\,\text{dB}$ and $L_{dipl} = 2\,\text{dB}$). As can be seen, transmit power is not excessive, considering 10 calls are being supported per aircraft. If the effects of imperfect power control were taken into account, the EIRP would be somewhat higher.

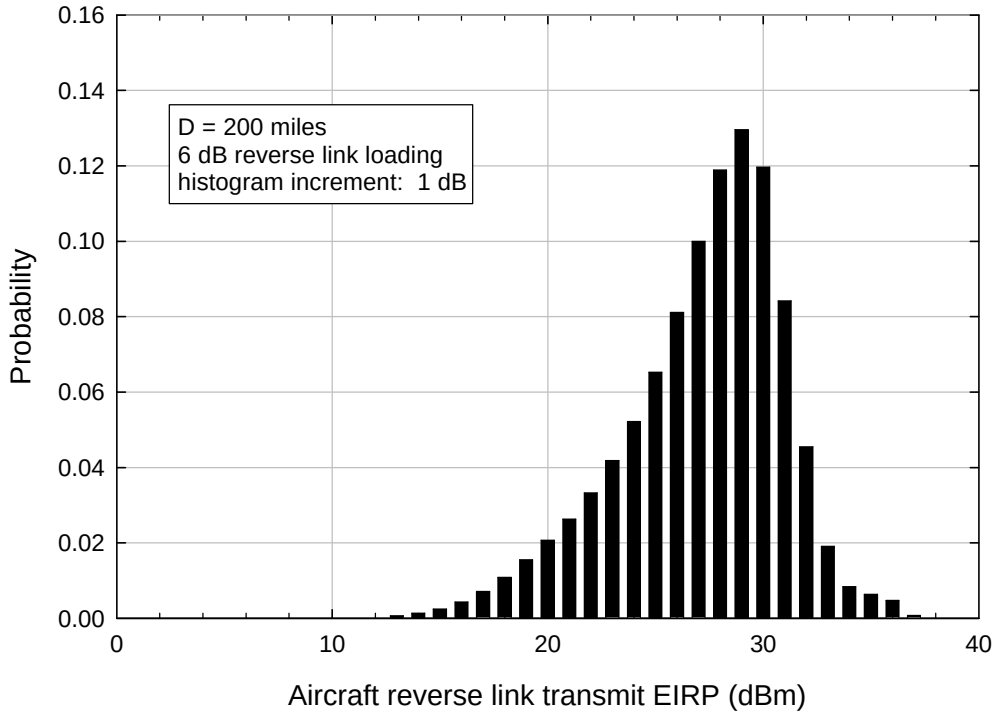

Figure 24: *Aircraft EIRP histogram with* $M_{sys} = 10\ dB$ *and* $L_{dipl} = 2\ dB$.

3.6. Comparison of Simulation Results with Analytical Approximation

When using simulations to study a complex process it is often useful to develop an analytical model that can generate independent results. These can be used to validate the simulation results for selected cases, and to provide physical insights into dominant effects and sensitivities. Such a model has been developed here for the SIR, and is described in detail in Annex C. With this model, a cell coverage area is approximated as a circle centered on the base station associated with the victim aircraft. Free space propagation is assumed, altitude is ignored, base station antenna gain is assumed constant, independent of the location of the aircraft, and outer-cell (same system) interference is approximated as a constant. The path loss between the victim aircraft and its desired base station, the power transmitted by each interfering aircraft, and the path loss between each interfering aircraft and the victim aircraft are all represented as uniformly-distributed random variables. As shown by the results, making these approximations makes little difference in the end results. For example, Figure 25 (same as Figure 53 in Annex C) shows the results for the circular cell approximation for the same link budget parameters as used in the simulation results. The parameter b is the outer-cell interference factor; that is, the outer-cell interference is b times the received desired signal at the cell edge. As can be seen, agreement with the simulation results discussed above is surprisingly good.

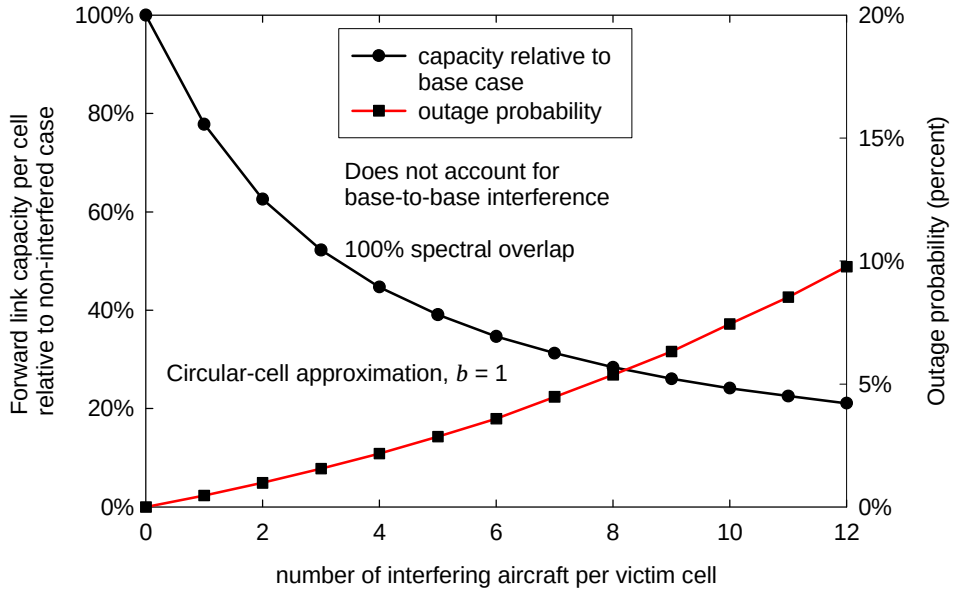

Figure 25: *Effect of cross-duplex interference, based on circular-cell approximation.* $b = 1.0$.

4. Simulation of Cross-Duplexed Systems under "Real World" Conditions

4.1. Introduction

The square grid simulation model developed above showed that it is possible for two cross-duplexed systems (system #1 and system #2) to coexist only under very optimistic ("sunny-day") conditions. When more reasonable aircraft transmit power levels or larger numbers of interfering aircraft per cell are assumed, there is a significant amount of interference received by a victim aircraft. Two questions then arise: 1) What impact do the non-idealities in a real system have on this conclusion? 2) Can we alleviate the effects of this detrimental interference through use of sectored base stations or a sectored aircraft antenna system?

A simulation framework is developed in this section that attempts to more closely model a real air-to-ground communication network than was done using square grid simulation above or in AirCell's work. To that end, several factors were included here to make the simulation reflect situations that would occur in the real-world, these include:

1. Non-uniform geographical distribution of air-traffic.
2. Sectored base station antenna patterns of commercially available antennas.
3. Sectored antennas on the victim aircraft with a best-beam selection system.
4. Actual existing base station locations.

Before providing a detailed description of the simulation parameters and methodology, it is instructive to first consider factors that will affect the simulation results. Since the air-to-ground and ground-to-air frequency bands are reversed in this situation, there will be interference occurring from one aircraft to another (air-to-air interference) and from one base station to another (base-to-base interference). For purposes of simplicity, in this simulation we ignore the base-to-base interference. In reality, however, the potential for base-to-base interference is significant, as was discussed above. We will concentrate exclusively on the air-to-air interference in the following subsections and in the associated simulations. Since, as was assumed above and in the AirCell analysis, we will be considering both systems to be 1xEV-DO type systems, an aircraft belonging to system #1 (victim aircraft) will have three sources of reception:

1. A signal from its serving base station.
2. Signals from non-serving base stations of system #1.
3. Signals from nearby aircraft belonging to system #2 (interfering aircraft).

The first signal in the above list will be considered the desired signal. Signals received from non-serving bases stations will be considered interference, since in 1xEV-DO systems, soft-handoff is not possible. Signals from nearby aircraft will also be

considered interference. The amount of interference from nearby system #2 aircraft will be determined by the distance to these aircraft, and the power level at which they are transmitting. The maximum power transmitted by an interfering aircraft is related to the signal-to-interference-plus-noise ratio (SINR) at the system #2 base station communicating with this aircraft. The actual power level depends on several factors, such as the traffic load on system #2, the amount of fading experienced, the nominal cell radii, and interference received by system #2 base stations from other sources.

Since the two systems do not fully overlap in the frequency-domain, each aircraft will only receive a portion of the full interfering signal. The amount of overlap between the two idealized frequency bands is 40%. However, these idealized concepts of bands show the energy outside of the allocated areas as reduced to zero. For any real commercial off-the-shelf 1xEV-DO CDMA equipment, there will be emissions outside the 1.25 MHz band. A stylized view of the idealized and more realistic spectral characteristics of the two systems is shown in Figure 26.

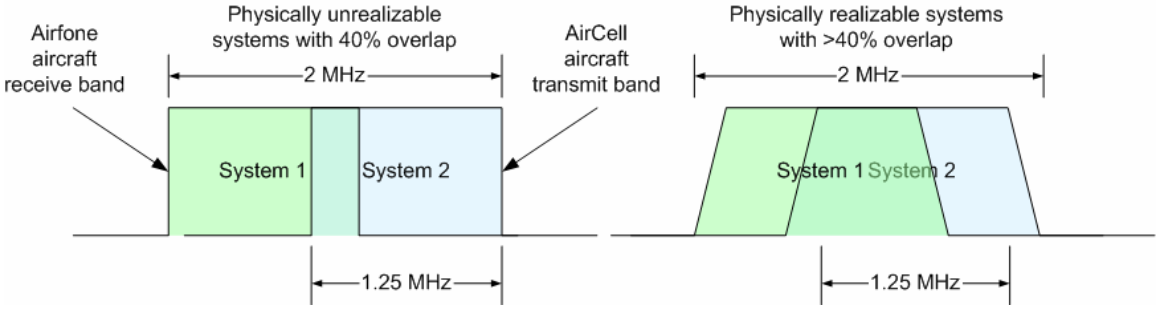

Figure 26: *Stylized representation of unrealizable (left) and realizable (right) spectral characteristics of COTS 1xEV-DO systems.*

To be conservative, an overlap value of 40% was used in the simulations even though a more realistic value would be higher.

4.2. Air traffic density and distribution modeling

In order to model the influence of transmissions from system #2 aircraft on the reception of signals at aircraft of system #1, we first need to know how many aircraft belonging to system #2 will be in the air at any one time. A first approximation can be made as follows. There are approximately 4,000 commercial aircraft in service, of which 60% are in the air at any time [4]. There are approximately 8,000 private aircraft, of which 20% are in the air at any time [4]. This leads to 4,000 aircraft in the air that could be equipped with an air-to-ground (ATG) communication system. This estimate was verified by viewing live flight information on Monday, May 17th 2004 at 5 PM EDT using the *AirNav Live Flight Tracker* software [6], which accesses a database of in-flight, landed, and planned flights in real-time. A screen shot of flights at this time is shown in Figure 27, with each aircraft represented as a green dot on the map.

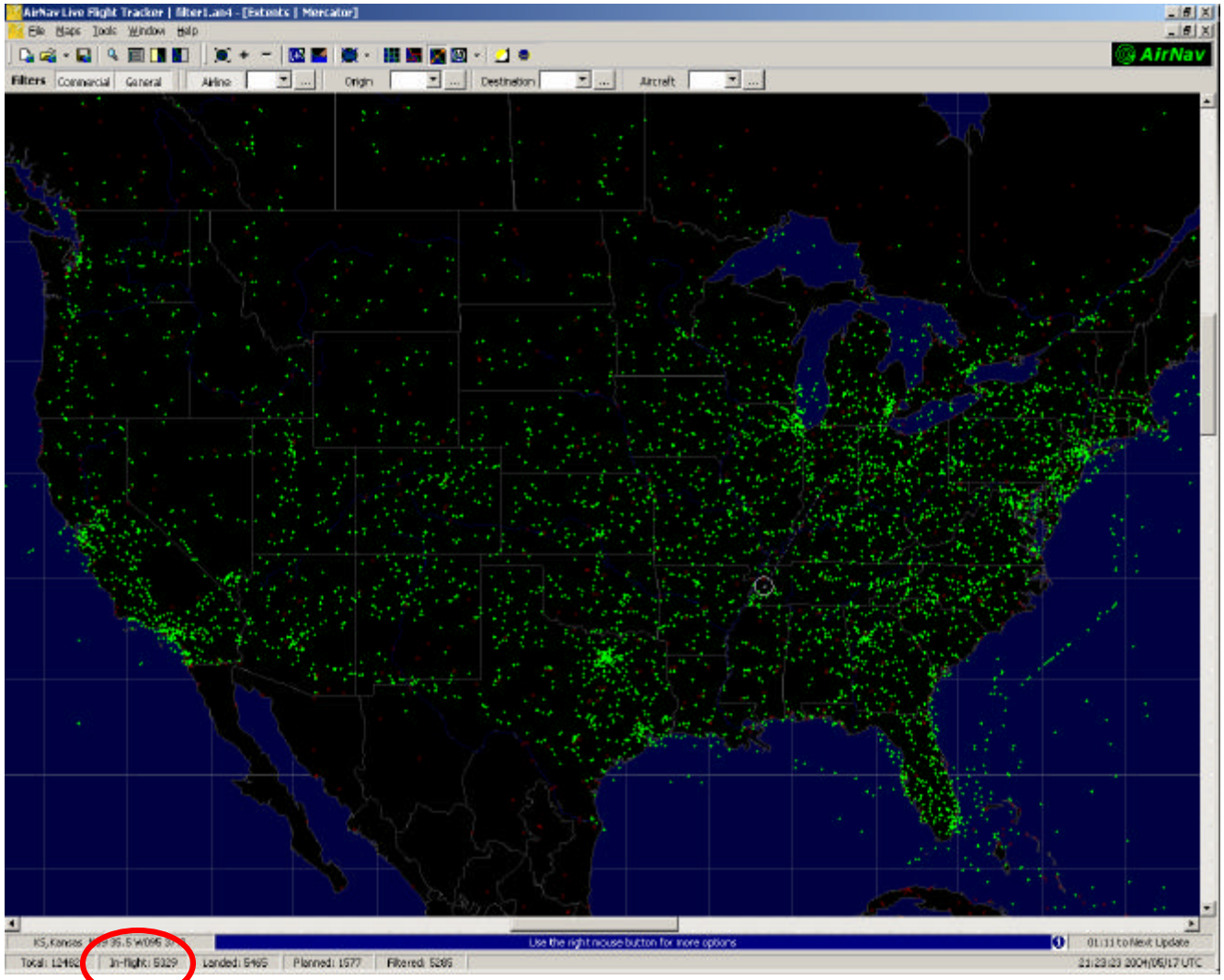

Figure 27: *Screen shot from AirNav Flight Tracker software showing all flights on Monday, May 17th 2004 at 5PM.*

The number of commercial and general aviation aircraft that are "in-flight" at this time was 5,329. This verifies that the rough estimate given above and used for the remainder of this analysis is of the right magnitude, but actually underestimates the number in-flight at peak times. This will make the Monte Carlo results be somewhat more optimistic than can be expected at peak air-traffic times. Also note that the non-uniform distribution of these actual in-flight aircraft roughly matches that of the Monte Carlo simulation shown in Figure 28 with very high densities of aircraft around the major airports on the east and west coasts.

As an example of how the 4,000 aircraft can be split among competitors, we can assume that the two major ATG providers are the system #1 and system #2 providers under consideration here. If these carriers split the addressable market of 4,000 aircraft, each will have 2,000 aircraft equipped with ATG systems at any time. From the point of view of any aircraft belonging to system #1 (victim aircraft), of the 2,000 interfering aircraft in the air at any time, those that are within the radio horizon of this victim aircraft will contribute to the total interference level.

Once we have established the number of interfering aircraft in the air at any time, we must determine the distribution of these aircraft. Since these flight paths originate and terminate at major airports, it is reasonable to assume that there will be a higher density of aircraft near these airports than anywhere else. Not only will more aircraft be taking off and landing, there will be many crossings at these locations.

The air traffic model assumed for purposes of this analysis consists of two components, a first component distributed uniformly over the continental United States and a second component with aircraft clustered around major airports. To determine the number of aircraft associated with each of these major airports we can use published information [7] that states that there is approximately 1 takeoff and 1 landing per minute at Newark International Airport (EWR). Using average approach and climb-out speeds of a 737-400 (~200 mph) this leads to an average aircraft spacing of approximately 4 miles. Therefore, in a 100 mile radius around EWR, we have approximately 50 aircraft. We can now use published statistics on passenger movements for the major airports from the year 2001 [8] to scale this number to match statistics for other airports. For example, EWR had 30,558,000 passenger movements in 2001, whereas Atlanta (ATL) had 75,858,500. Since EWR has 50 aircraft associated with it in a 100 mile disk, ATL will have approximately 2.48 (75858500/30558000) times that number, or 124 aircraft within that same size disk. A table listing these numbers for some major airports is shown in Table 3. The total number of aircraft out of 4,000 that are associated with all of these major airports is 1,435. This leaves 2,565 distributed uniformly across the rest of the continental US. Another constraint is that the interfering aircraft are to be placed no closer than 5 miles to any other aircraft.

For the following simulations, the distribution of aircraft around each of the airports was uniformly distributed in radius (up to 100 miles) from the airport and uniformly distributed in angle (between 0 and 360°) centered about the airport. Also, since we would like to model a varying number of interfering aircraft of up to 50% market share

(2,000 aircraft), we can generate 4,000 aircraft using the methodology discussed above and then randomly choose any number we need (<4,000). One distribution, or laydown, of the appropriate number of interfering aircraft will be used for a single Monte Carlo trial associated with one location of the victim aircraft. The locations of the victim aircraft will be chosen by this same method, also with the constraint that no interfering aircraft can be within 5 miles of the victim aircraft.

Table 3: *Aircraft associated with major North American airports.*

Airport	Aircraft within 100 Mile radius
ATLANTA (ATL)	124
CHICAGO (ORD)	110
LOS ANGELES (LAX)	101
DALLAS/FT WORTH (DFW)	90
DENVER (DEN)	59
PHOENIX (PHX)	58
LAS VEGAS (LAS)	58
HOUSTON (IAH)	57
SAN FRANCISCO (SFO)	57
MINNEAPOLIS/ST PAUL (MSP)	56
DETROIT (DTW)	53
MIAMI (MIA)	52
NEWARK (EWR)	50
NEW YORK (JFK)	48
ORLANDO (MCO)	46
TORONTO (YYZ)	46
SEATTLE (SEA)	44
ST LOUIS (STL)	44
PHILADELPHIA (PHL)	43
BOSTON (BOS)	42
BALTIMORE (BWI)	41
REAGAN (DCA)	40
DULLES (IAD)	39
LAGUARDIA (LGA)	39
HARTFORD (BDL)	38

A sample geographical plot of 2,000 interfering aircraft is shown in Figure 28, where each blue dot represents one aircraft.

It should be noted here that this distribution is only an approximation of the actual distribution of aircraft over the continental US at any one time. The actual geographical distribution will have aircraft constrained to be located within pre-determined flight lanes. The distribution chosen above will lead to more conservative SINR results than would be experienced in reality. This is because a victim aircraft constrained to a flight

lane with the interfering aircraft will have an average distance to its closest neighbors that is smaller than would be the case with the mostly uniformly distributed interferers.

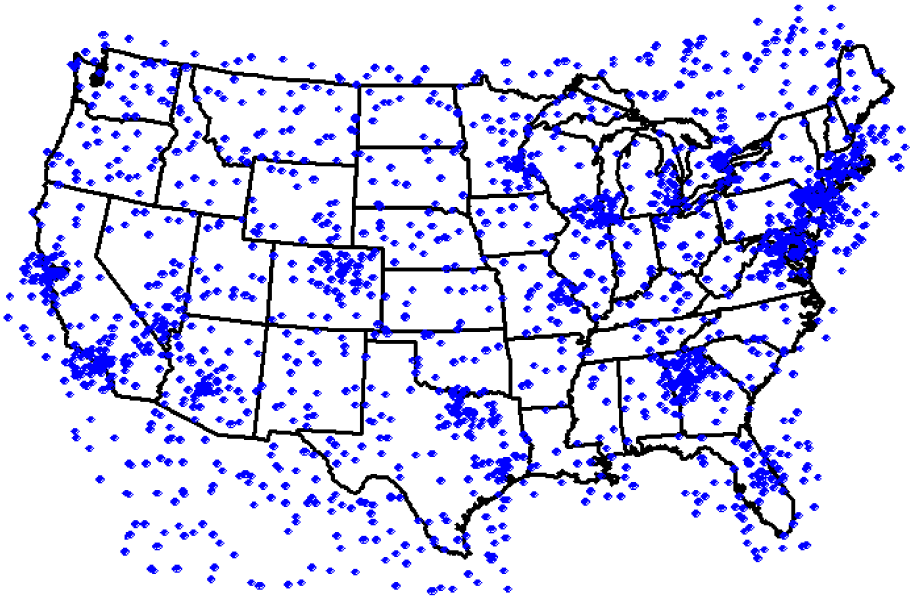

Figure 28: *Geographical distribution of 2,000 aircraft over the continental US.*

4.3. Victim Network Characteristics

The victim network is assumed to be a 1xEV-DO type network with 3 sector base stations located where current Airfone narrowband base stations exist [4]. These locations are shown in Figure 29 as red dots on the map.

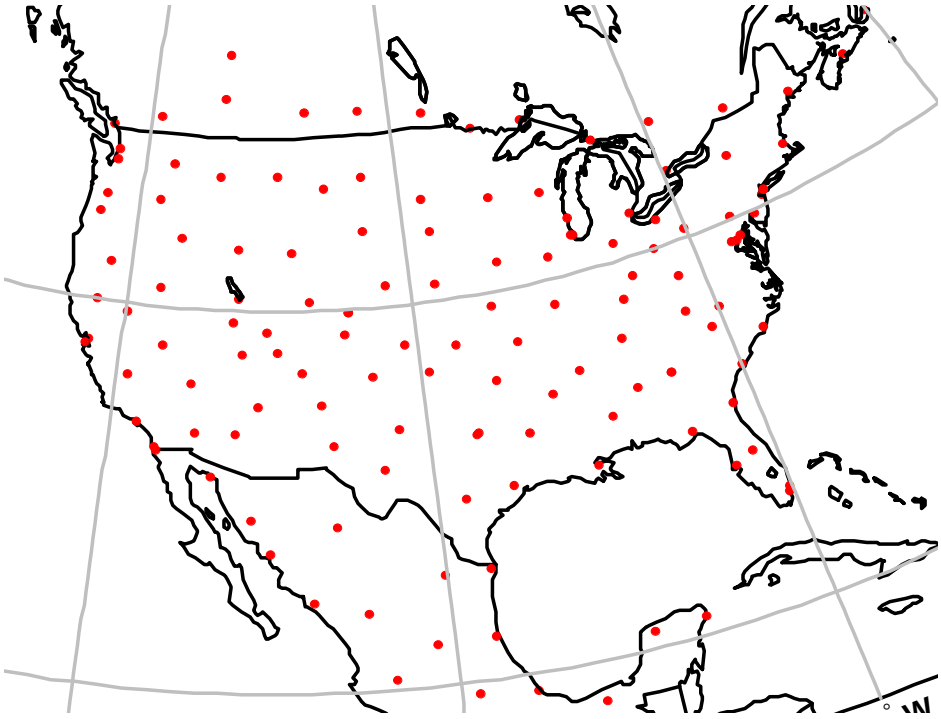

Figure 29: *Location of victim network (system #1) base stations.*

All of the base stations shown in the figure are identical and all have the following physical characteristics:

- All base stations transmit at constant 43 dBm power output from the transmit power amplifier (PA).
- 5 dB miscellaneous losses between the ground PA and antenna.
- Each base station is configured as a 3 sector site with sectors oriented 0°, 120°, 240° from true north.
- Antenna patterns used (both azimuth and elevation) are from commercially available base station antenna with 5 degree electrical uptilt (actual patterns are shown in Figure 30). This antenna has boresight gain of 15 dBi.
- 10 dB of system implementation margin was assumed for paths joining each base station to the victim aircraft, i.e., a uniform random variable (in dB) was chosen to account for misc. losses associated with antenna pointing errors, fading, losses from obstructions, and other possible impairments.
- All base station towers are 100 feet tall.

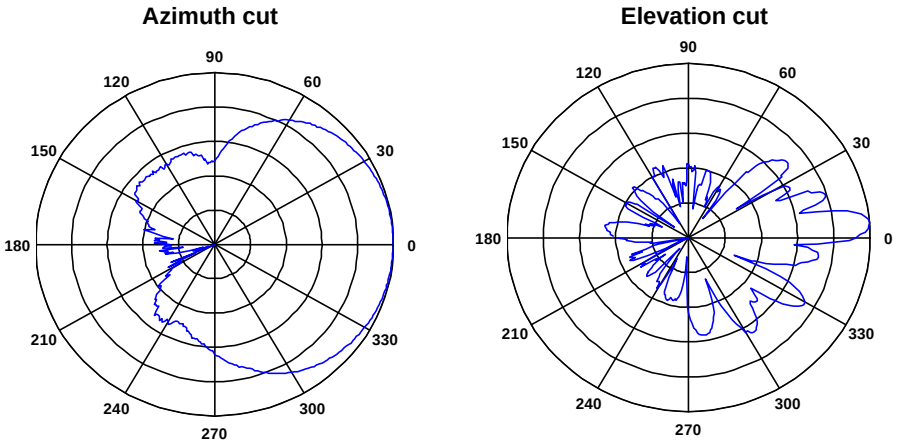

Figure 30: *Azimuth and elevation cut of base station antenna patterns used in the simulations.*

The aircraft from system #1 (victim aircraft) are assumed to possess a switched-beam antenna system in order to combat self- as well as other-system interference. A switched-beam antenna system is one where, instead of having an omni directional antenna covering the 360° of azimuth, several (6 in this case) antenna beams are formed using multiple antenna elements and a Butler-matrix to sectorize space. The antenna system continually monitors the SINR on each beam and uses an *N*-way selector switch to choose the best beam for communications. A stylized representation of an example eight-beam switched antenna system is shown in Figure 31.

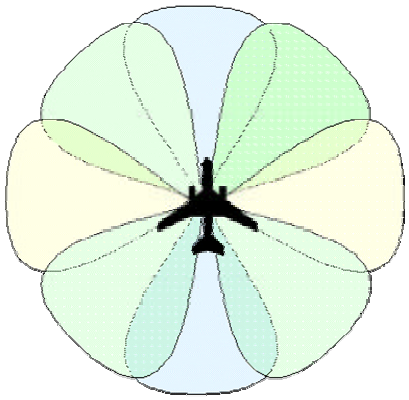

Figure 31: *Switched-beam system antenna beam layout showing sectorized patterns.*

To simplify the simulations, a "keyhole" azimuth sector pattern was used on the aircraft. This ideal keyhole antenna pattern is shown in Figure 32.

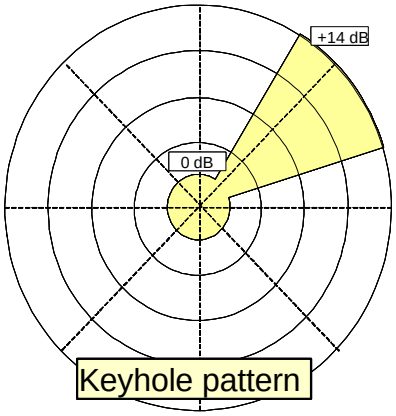

Figure 32: *Keyhole antenna pattern.*

The boresight (or maximum) gain was taken to be 14 dBi, with a front-to-back ratio of 14 dB, resulting in a gain of 0 dBi outside the main beam. The elevation pattern was assumed to be uniform over all elevation angles.

The antenna system used in the simulation was a six-beam system with beam number 1 pointing in the direction of aircraft heading (random heading was used for each laydown). Beam number two points 60° clockwise from beam number 1, and so on. Losses of 5 dB are used after the antenna to account for cabling, diplexer, and other miscellaneous losses. A noise figure of 7 dB is also used at the aircraft.

All victim aircraft were placed at 35,000 feet with a radio horizon to the 100 foot base station towers of 278 miles. Note, that the radio horizon in miles is approximately:

$$R_{horiz} = \sqrt{2}\left(\sqrt{h_1} + \sqrt{h_2}\right) \tag{6}$$

where h_1 and h_2 are the heights of the end points (base station and aircraft here) in feet. The victim aircraft are placed randomly using the same geographical distribution as discussed in Section 4.2.

4.4. Interfering Network Characteristics

The interfering network is assumed to also be of 1xEV-DO type. The number of aircraft present in system #2 is used as a parameter for the simulations to show how the effect of interference varies with interfering aircraft density. Since no information was known about locations of system #2 base stations, they are assumed to be randomly located throughout the country. This random location of base stations is accomplished indirectly by letting the power level transmitted from each of the interfering aircraft be a random

variable with a certain distribution. The distribution of powers for each aircraft in the collection of interfering aircraft is determined by the type of power control scheme used. For the following simulations, it is assumed that all of the interfering aircraft have perfect power control and that aircraft associated with the best server are distributed in a circular disc centered at the base station. Power control works by maintaining a constant received power from all aircraft belonging to a base station. For this disc arrangement, the probability that an aircraft's horizontal distance to its serving base station is less than some chosen value *y* is

$$\Pr(d < y) = \frac{y^2}{D_{\max}^2} \tag{7}$$

where D_{max} is the maximum cell radius. Since we are using a free space path loss model for air-to-ground communications here, the transmitted power must be proportional to the square of the distance to exactly balance the d^2 path loss and maintain the same signal level at the receiver. That is, transmitted power can be written

$$P_{tx} = kd^2 \tag{8}$$

The path loss is considered to be free-space and the received power at a distance *d* can be found using the radar equation [9]:

$$P_{rx} = \frac{G_1 G_2 L \lambda^2 P_{tx}}{(4\pi d)^2} \tag{9}$$

where G_1 and G_2 are the antenna gains of the ground and aircraft antennas along the line joining the aircraft and base station, *L* is miscellaneous loss, λ is the radio wavelength in free space, and *d* is the distance between base station and aircraft.

The proportionality factor *k* (or equivalently, the target receive power P_{target}) is chosen so that the power received at the base station is enough to maintain the reverse link at the designed maximum distance from base station (cell edge), P_{target}, i.e.,

$$k = \frac{(4\pi)^2 P_{\text{target}}}{G_1 G_2 L \lambda^2} \tag{10}$$

If the transmitted power is proportional to the distance squared as in (8), and using the known CDF for distance given in (7), the probability that the transmitted power is less than a chosen value *v* is written as

$$\Pr\left(kd^2 < v\right) = \frac{v}{kD_{\max}^2} \tag{11}$$

Differentiating the CDF in (11) gives a uniform distribution of power in Watts and an exponential distribution of power in dBm. A sample of this distribution is shown in Figure 33.

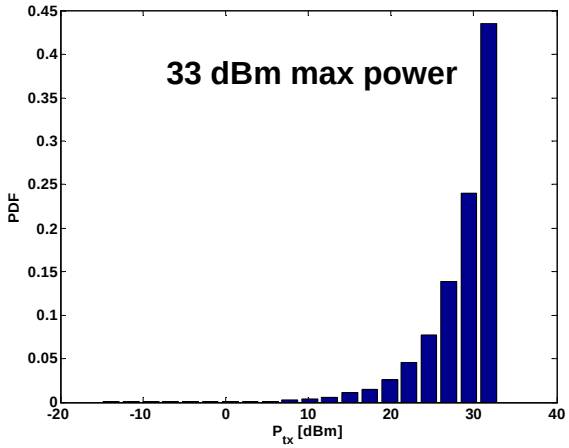

Figure 33: *Sample transmit power distribution for interfering aircraft with 33 dBm maximum power.*

In order to arrive at the correct maximum transmit power for the interfering system, a link budget can be constructed that accounts for all of the various system gains and losses. An example link budget at a cell edge of 250 miles for a 75% loaded system is shown in Table 4. This table demonstrates that the minimum required transmit power needed to close the reverse link at the cell edge for a 96 kpbs total reverse link throughput (for the entire aircraft) is 33 dBm. If 10 users were using the air-to-ground data service at the same time, this would correspond to only 9.6 kbps per users of raw data rate. If the data rate were increased, the required power would increase proportionally, assuming the E_b/N_t requirement and the noise plus interference at the receiver remain the same.

The cell edge power corresponds to the maximum of the power distribution shown in Figure 33 for a system using power control. A point to note for comparison is that a single handheld cellular phone's maximum transmit power is 23 dBm. Another point to note is that for the values used in the table, the reverse link barely reaches the target E_b/N_o (actually it is slightly below the target, but because this is an approximate result, -0.5 dB is taken to be close enough to the target). A 10 dB system implementation/fading

margin was assumed as is typically done during planning of the air-to-ground network [4]. This margin is included to take into account antenna mounting accuracy, higher than expected cable loss, fading due to blockage, and other unexpected design losses. This 10 dB seems reasonable considering all of the unknown factors that come into play when designing a system that needs to operate robustly. It is possible to reduce this number and obtain much more optimistic results. However, the resulting robustness of the system may suffer. If no system implementation/fading margin is included, all that is required for the system to stop operating or to begin operating poorly is to have a stand of trees in the line-of-sight to the aircraft, or have a large ground reflection component. Neglecting a system implementation/fading margin would result in a fragile network with service that is likely to be unacceptable compared with the quality of service currently expected and experienced by mobile communication customers.

Table 4: *Example reverse-link budget for interfering system with 96 kbps from aircraft.*

Air-to-ground link budget

Aircraft	Ptx at antenna connector	33	dBm	
	Air antenna gain	0	dBi	
	Air EIRP	**33**	dBm	
Channel	distance	250.0	miles	
	freq	895	MHz	
	Free space path loss	**143.6**	dB	
	Fading margin	10	dB	
Base station	Ground antenna gain	15	dBi	
	Cable, diplexer, etc. losses	5	dBi	
	Prx at receiver	**-110.6**	dBm	
	Bandwidth	1.25	MHz	
	Noise figure	4	dB	
	Noise power	**-109.0309**	dBm	
System	System loading	75%		
	Noise rise (self)	**6.0**	dB	
	Noise rise (other)	0.0	dB	
	Data rate	96	kHz	
	Chip rate	1.2288	MHz	
	Processing gain	**11.1**	dB	
	Eb/No target	4	dB	IS-2000 target
	Eb/No at base station	**3.5**	dB	
	Margin	**-0.5**	dB	

4.5. Simplified Interference Example

Before describing the statistical Monte Carlo methodology and the results generated, we would like to present a simplified example using concepts explained above to demonstrate how serious interference conditions can occur with the cross-duplexed concept.

Consider the situation shown in Figure 34. There are three aircraft flying near each other (5 mile spacing) on the same, or close, flight paths. The base stations that are serving these aircraft are located near the same airport (as is likely to happen). The system #1 aircraft is 150 miles from the airport and the two system #2 aircraft are 145 and 155 miles from the same airport. Using the same parameters as shown in Table 4, but with distances as described above, we find that the SINR as seen at the victim (system #1) aircraft is -18 dB. This means that the victim aircraft is well below the required SINR to maintain a call (-12.5 dB is the minimum level needed). As the aircraft fly along the flight path the SINR improves somewhat if they are closer to the base stations. However, as they get farther from this base station, the problem is exacerbated.

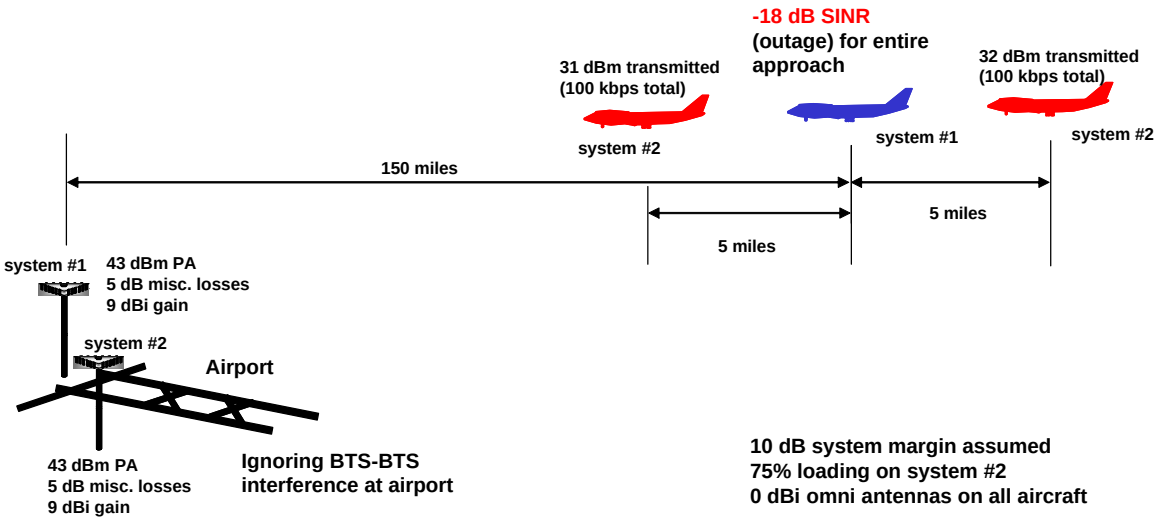

Figure 34: *Example scenario with victim aircraft experiencing an outage.*

It is possible then, to experience poor service quality, or outage, along an entire flight path if interfering aircraft are also flying along that flight path. This case might not occur frequently, but when it does occur no one on the aircraft can use the data services.

It is possible that as the aircraft altitudes vary with respect to each other, some degree of fuselage shielding can be expected. However, the amount of shielding to be expected varies widely with the type of antenna used, its position, and the shape and size of the aircraft. Additionally, the range of angles between aircraft is not expected to be large,

since aircraft are restricted to cruising altitudes (between approximately 28,000 and 40,000 feet). With the minimum separation of 5 miles, the maximum angle from the horizon between aircraft is expected to be about 24°. At this angle, some degree of shielding can be expected, but the amount is very variable. Also, the maximum shielding only occurs when one aircraft is at the top of the cruising range and the other is at the bottom. There will be a wide distribution of altitudes, and this worst case example was not meant to show how likely a disastrous situation is, but that it is possible to have a situation where communication on the victim aircraft is eliminated for a large portion of a flight due to interference.

The Monte Carlo simulation presented next will address the question of degradation of service on average for many possible cases over the continental US.

4.6. Monte Carlo Simulation Methodology

The Monte Carlo simulation methodology proceeds as follows:

- Place the specified number of interfering (system #2) aircraft across the continental US, randomly located according to the non-uniform distribution discussed in Section 4.2.
- Place a single victim (system #1) aircraft, possessing six antenna beams, randomly located with position taken from the same distribution.
- For beam *n* of the 6 aircraft antenna beams:
  - Calculate the received signal strength using free space path loss to all of the system #1 base stations within the radio horizon.
  - Choose the base station with the largest received signal strength (smallest path loss) as the serving base station. This is the desired signal.
  - Calculate the received signal level from all other, non-serving, visible system #1 base stations. These signals are considered interfering signals.
  - Calculate the received signal level from all visible interfering (system #2) aircraft. These signals are also interfering signals.
  - Calculate the SINR for beam *n*.
  - Repeat for all beams.
- Record the SINR for that location as that from the beam with the best SINR out of the 6.
- Repeat for the specified number of iterations (laydowns).

Once this process is repeated for the specified number of laydowns, we have a collection of SINR values associated with locations across the continental US. Since the SINR is a random variable, we can examine its cumulative distribution function and other

statistical properties. A sample CDF of the system-wide SINR for the victim system with 2000 interfering aircraft present over the entire continental US is shown in Figure 35

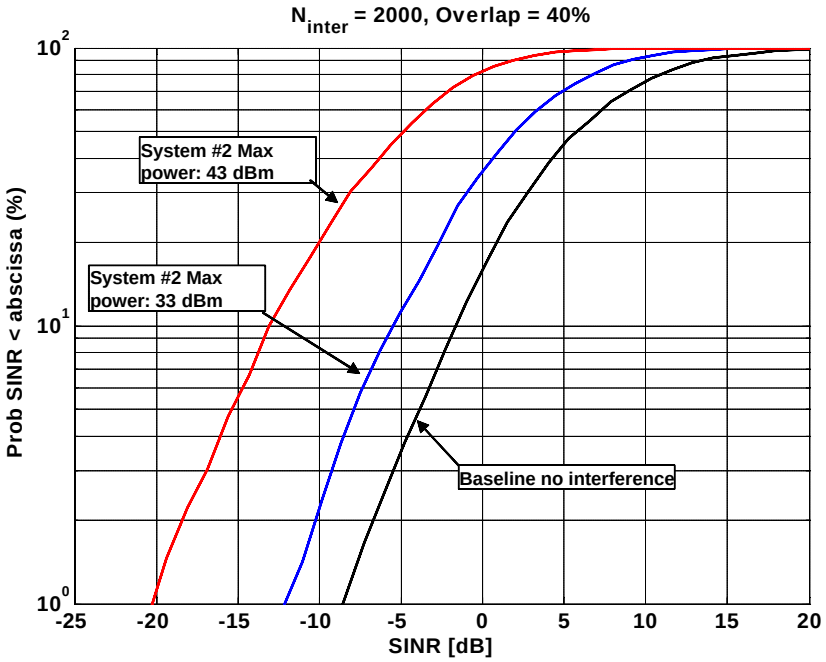

Figure 35: *Sample CDF of SINR with different interfering aircraft maximum powers.*

We can also map the SINR values to expected throughputs for a 1xEV-DO type system through a table or by using an approximate continuous mapping. As shown in Figure 36, the 1xEV-DO SINR to data rate (throughput) mapping can be approximated by shifting the Shannon bound curve to the right by a 4 dB offset. In reality, the curve would be a stair step curve with levels specified by the black squares in the plot, but the continuous curve provides a finer granularity of results.

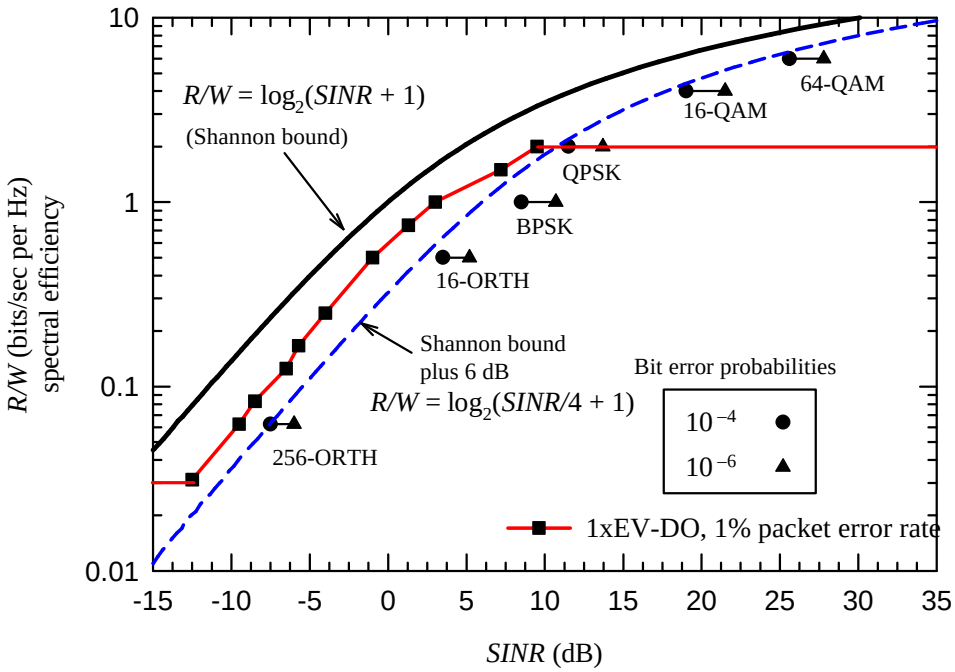

Figure 36: *SINR to throughput mapping for 1xEV-DO and approximate continuous curve.*

4.7. Results

Simulations were performed using the methodology described in Section 4.6 and with the assumptions put forth in Sections 4.2–4.4. The parameters that were varied to judge the effect of system #2 interference were the number of interfering aircraft over the continental US at any time and the maximum transmitted power of each of these aircraft. Recall that power control was simulated on these aircraft and the power level indicated in the results reflects only the maximum possible power, and actual power transmitted by each interfering aircraft will be less than this value with probability as given in Figure 33.

The range of the number of interfering aircraft present is 150–2000. The large range of values was chosen to show that at the lower end of the range, with a very lightly loaded interfering system, the performance of system #1 is essentially unaffected. This is an unrealistic scenario, however. As system #2 initially launches service, number of subscribing airlines is expected to be low and interference into an existing system #1 should be minimal. As the market share for system #2 grows, its presence will significantly affect service for system #1. Also, since we have assumed the cross-duplexed band concept here, system #1's presence will also significantly affect service for system #2.

In order for the second system to operate effectively, it must have a number of base stations that is approximately equal to the number of base stations belonging to system #1. To see why this is the case, consider the situation where system #2 has a small number of base stations, while system #1 has a large number. If there is an addressable market of 4,000 aircraft, and system #2 only has a small number of base stations, it can only serve a very small fraction of these aircraft. Hence, within any chosen volume in the air, there will be many more aircraft from system #1 than from system #2. This implies that there will be large amounts of interference from aircraft of system #1 into the receivers of aircraft from system #2. Also, since system #2 has a small number of base stations, but needs to cover the entire country, each of its aircraft will be very far from a serving base station, on average. This will result in very low SINR conditions, and possibly many outages, for system #2. Therefore, system #2 must have a similar number of base stations as system #1 in order to keep the signal level from serving base stations high to maintain cross-country continuous service.

If we assume that the total addressable market for air-to-ground service is 4,000 aircraft as explained in Section 4.2, then we can relate the number of interfering aircraft to the market share for system #2, where 2,000 aircraft represents 50% market share for the interfering system. Since there are approximately 150 base stations used by system #1, we expect system #2 to have 150 base stations, also. With 2,000 aircraft belonging to system #2, this represents about 4 aircraft per sector for a 3 sector system.

The other parameter that is varied is the maximum transmitted power from each of the interfering aircraft. Two values were chosen, 33 dBm and 43 dBm. As was shown in the reverse-link budget shown in Table 4, 33 dBm is needed at a 250 mile cell edge to achieve 96 kbps of reverse-link throughput. Remember that this is 96 kbps shared among all users in an aircraft of the reverse link. If there are 10 users, they will each receive 9.6 kbps throughput on average. At this level of per-user throughput, this cannot really be called a broadband service. A higher data rate will require more power, and to achieve rates comparable to those available on the forward link, it is reasonable to expect that a comparable transmit power level will be needed (e.g., 43 dBm).

Figure 37 shows the geographical distribution of expected SINR at system #1 aircraft for the baseline case, or the case with no interferers present. The colors of each dot represent the SINR level, and the legend at the bottom shows how color maps to SINR. When the color of a dot is black, it means no service is possible. The secondary scale below the SINR scale shows the achievable data rate corresponding to that SINR. It is seen that service is generally good, with few outages, except near major airports, where there may be several base stations within view. Since this is a CDMA system, these base stations contribute to the interference level.

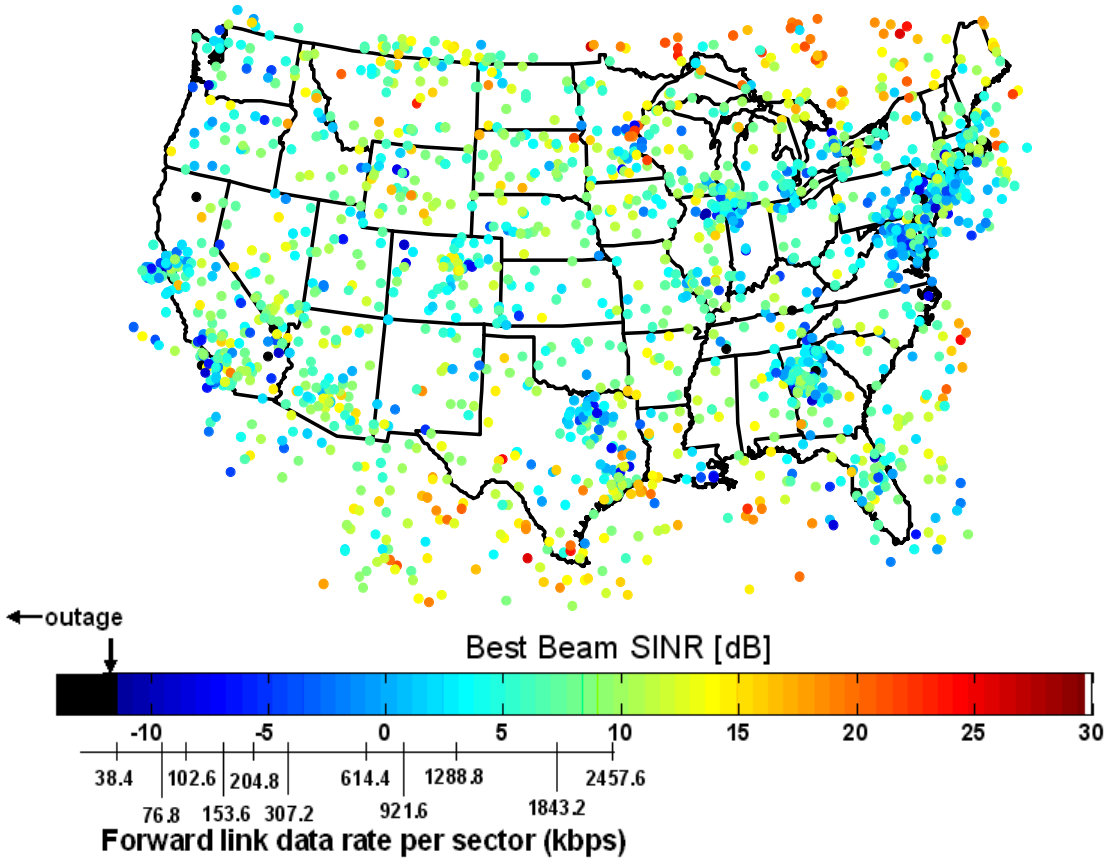

Figure 37: *Geographical distribution of SINR with no interferers present.*

When system #2 achieves 50% of the market share, there will be approximately 2,000 aircraft belonging to system #2 in the air at any time. When each of these aircraft can radiate at most 43 dBm, the geographical distribution of SINR at a system #1 aircraft becomes what is shown in Figure 38. It is obvious that performance has significantly degraded throughout the country. There are many outage areas, especially near the airports.

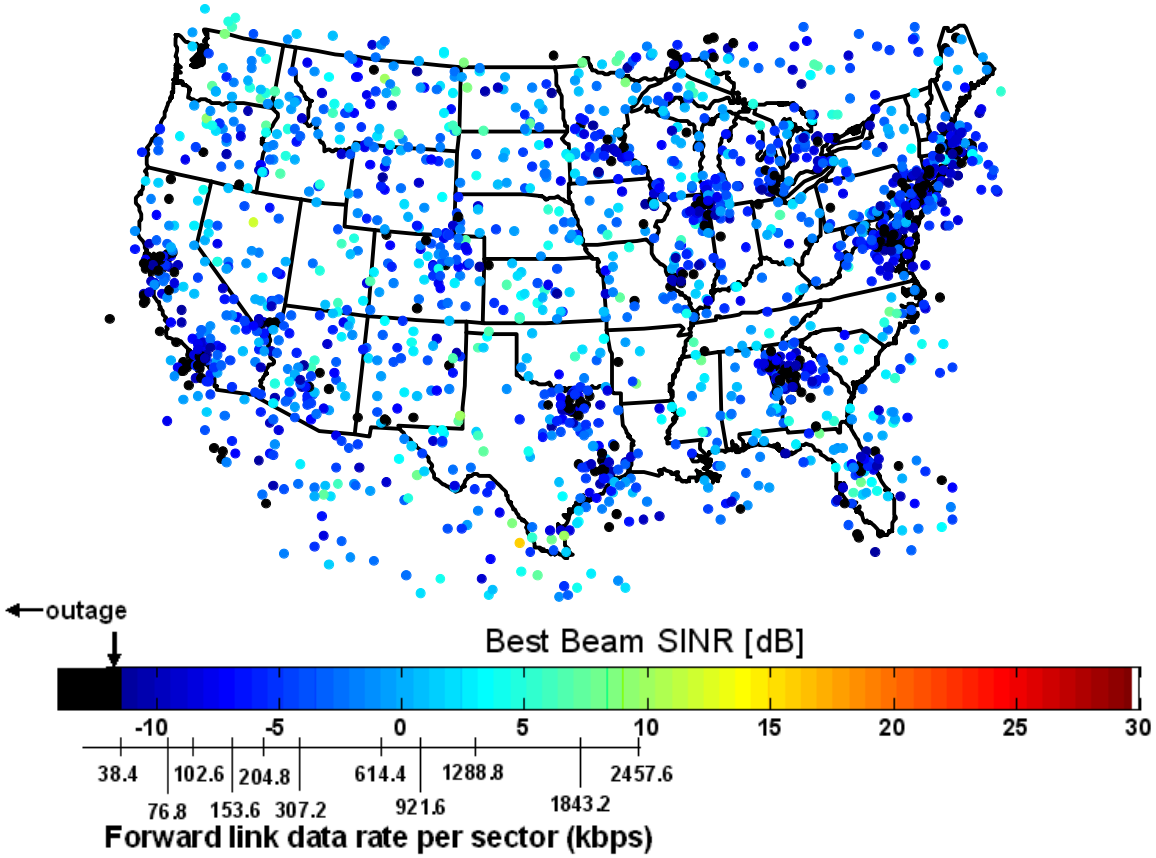

Figure 38: *Geographical distribution of SINR with interferers.*

A measure of the quality of service for a wireless system is the outage probability, or the probability that the SINR does not achieve even the minimum allowable value, and the link is broken. For 1xEV-DO, the SINR value where this occurs is -12.5 dB. Below this SINR, no service is achievable. Remember that when an outage occurs, no service is achievable on the entire aircraft. A plot relating outage probability versus the number of interfering aircraft on system #2 for two different maximum transmit powers on the interfering aircraft is shown in Figure 39. As can be seen in the figure, even when the maximum transmit power per interfering aircraft is kept below 33 dBm (corresponding to a low reverse-link data rate per aircraft), the outage probability doubles when a very small number of aircraft are present on system #2 (left side of the curve). When system #2 reaches 50% of the market, the outage probability increases by 7.5 times (750%) over the baseline case with no interferers present.

When a more realistic power level for two-way broadband services (43 dBm) is used for each interfering aircraft, the results are much worse, with the outage probability increasing by a factor of 50 (5,000%) when system #2 has 50% of the market.

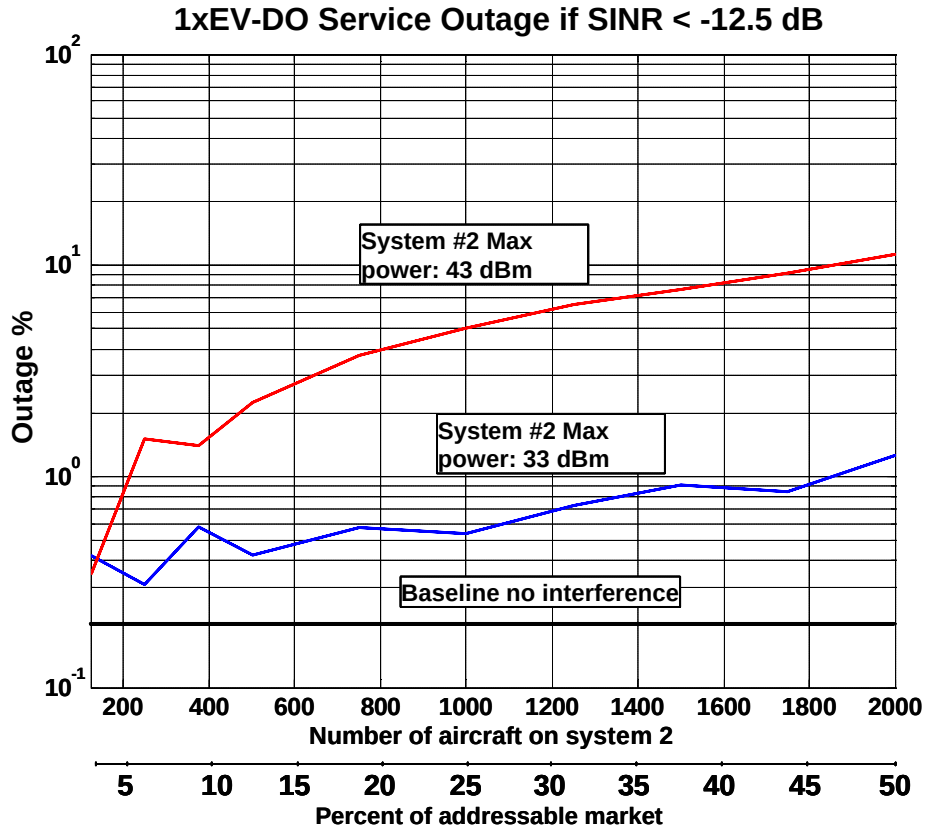

Figure 39: *Outage probability as a function of system #2 market share for two different interferer aircraft maximum transmit powers.*

To see how the degradation in SINR across the network reduces the data throughput, we can plot the mean throughput per sector versus the market penetration of system #2 for varying interferer power levels (Figure 40). The figure shows that when system #2 has 50% of the market and is operating with a low reverse-link throughput (96 kbps per aircraft), the mean forward-link throughput per sector of system #1 drops from 1.7 Mbps to ~1.1 Mbps. However, when aircraft on system #2 transmit a higher power (higher reverse-link throughput), the mean forward-link throughput per sector drops to 400 kbps for system #1, that is a 76% reduction in throughput.

The results presented here are intended to model situations encountered at cruising altitudes with minimum spacing between aircraft of 5 miles. The interference between aircraft is even worse as the aircraft are closer together, as is the case on approach or climb-out. Any effort to minimize the probability of occurrence by, for example, prohibiting broadband operations below 10,000 feet would inhibit use of the service in other contexts such as on commuter aircraft and general aviation craft (particularly business planes) and for aircraft operational monitoring. Such a restriction devalues the service, and seems a high price to pay for the spectrum-sharing approach proposed by AirCell.

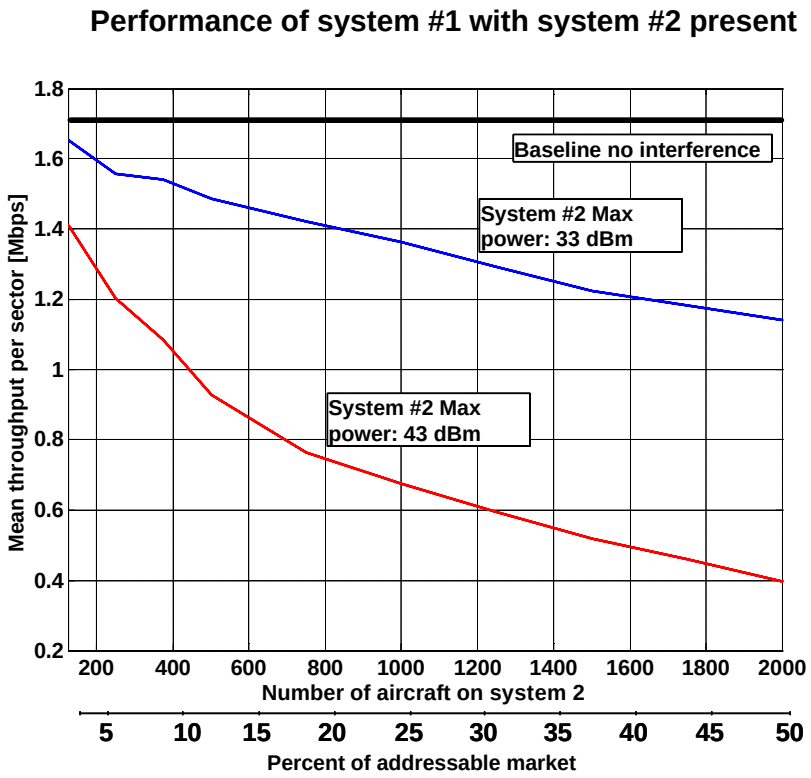

Figure 40: M*ean throughput per sector as a function of system #2 market penetration and power level.*

4.8. Conclusions

There are serious limitations associated with the reverse-duplexed proposal. Most notably, with just 2 interferers present along a flight path, the aircraft can experience an outage for the entire flight. A switched-beam antenna system simulation was performed in order to determine whether this interference mitigation technique could be used to allow two carriers with cross-duplexed bands (system #1 and system #2) to coexist within the same spectrum. It was found that outage probability increases to an unacceptable level (from 0.2% to >12% nationwide, with large outage areas near major airports). Forward link (ground-to-air) data rate drops significantly (from 1.7 Mbps to 400 kbps per sector).

AirCell has shown that with perfect textbook link budgets and aircraft transmit power limited to 200 mW, the aircraft-to-aircraft in interference is minimal with the cross-duplexed sharing concept. However, designing a system with no system implementation/fading margin is not common practice in the world of cellular/PCS network planning. Based on Airfone's previous design and planning experience, 10 dB of margin was deemed to be a reasonable value [4]. While AirCell's analysis concludes

that harmful interference would be minimal under "sunny day" conditions, such conditions would not normally apply in real-world situations. Our analysis and simulations demonstrate the significant and mutually harmful interference will occur between such competing systems.

Another important thing to note is that the degradation in the performance of one system is directly related to the success of the largest provider, i.e., when one of the systems gains market share, and hence has more aircraft in the air, the other system's performance is significantly degraded.

Additionally, although AirCell ignores it, base-to-base station interference in this scenario will be prevalent near any major airport as base station separations in these areas are generally much less than the radio horizon. In these cases, the interference will eliminate any possibility of communication between the base and aircraft.

While simulations presented here are meant to model the situations that occur near cruising altitudes, those situations encountered on climb-out or approach (below 10,000 feet) will inevitably be worse, due to the reduced distances between aircraft.
Any effort to minimize this probability of occurrence by prohibiting broadband operations below 10,000 feet would limit the range of application of this service; for example, the possibility of aircraft monitoring over this link would be eliminated.

All of these factors taken together indicate that such a cross-duplexed system is not viable in the ATG spectrum.

5. Effect of Naval Air-Search Radars on Reverse-Duplexed Aircraft Reception

The U. S. Navy uses the AN/SPS-49 air search radar aboard many of its warships, including all aircraft carriers. There are 48 frequency channels defined in the band 850-942 MHz. Typical peak transmit power is 360 kW and the antenna gain is 28.5 dB. Operational restrictions generally limit the use of the AN/SPS-49 within 200 nm of land to the 902-928 MHz ISM band [12] (which is also used by unlicensed devices under Part 15 of the FCC Rules). As detailed in [12] there are a number of coastal areas which are used for training on the AN/SPS-49 but "Based on past operational experience, an interference protection zone of 30 nm inland from coastal areas has been found sufficient for sharing with other services and is suggested to reduce interference in [the designated training areas]"([12], pp. 4-5). It is also mentioned that in a number of the areas, "terrain shielding should generally mitigate any potential interference from the subject radar."

Airfone's base stations in some of these coastal areas experience interference from the AN/SPS-49 with some regularity[4] [4]. Since the Airfone base stations receive in the 894-896 MHz band, it is reasonable to suspect that the interference is due to sidebands from an emission on a nearby channel within the 902-928 MHz band, as a ship more than 200 nautical miles offshore would be beyond the radio horizon of the base station.

However, with the duplexing reversed and an aircraft receiving in the 894-896 MHz band, as proposed by AirCell, the radio horizon to the ship is much greater – about 250 miles, and there will be no terrain shielding. The path loss for a 250 mile separation distance is about 143 dB. With an EIRP of 114 dBm from the radar, the power received by the aircraft is –29 dBm, minus a factor to account for spectral rolloff, which might reasonably be expected to be 60 dB or more far away from the center frequency, but much less near the center frequency (see, e.g., [13] for example radar emission spectra). Assuming a 30 to 60 dB range to account for spectral rolloff, the interfering signal received by the aircraft is –59 to –89 dBm. With a 6 dB noise figure, the noise floor is –107 dBm, so the interference is 18 to 48 dB above the noise floor of the aircraft receiver. For a lesser separation, the effect will be correspondingly more severe. For example, with a 50 mile separation the path loss is about 14 dB less and the interference would be in the range –45 to –75 dBm, or 32 to 62 dB above the noise floor.

It is therefore reasonable to expect that interference from the AN/SPS-49 will be a much more common problem for reverse-duplexed aircraft than it currently is for ATG base stations receiving in the 894-896 MHz band and will have a deleterious effect on any such system.

[4] As recently as May, 2004, radio base stations located near Charleston, SC and St. Simons Island, GA were completely saturated by suspected radar interference. The interference blocked all call processing. It was only after intervention by the FCC that service was resumed. Such occurrences have been observed regularly by radio base stations located on both coastlines.

6. Adaptive Antenna Issues for Multiple System Coexistence

6.1. Introduction

Boeing [11] has proposed use of adaptive antennas on all aircraft and base stations to alleviate interference problems in order to support multiple system sharing of the 850/895 MHz ATG spectrum. The proposed spectrum plan is shown in Figure 41. In this short technical note, we will show that unacceptable amounts of interference would result from a spectrum plan where multiple providers are allowed to overlap in frequency without the use of adaptive antennas. We will also show that reasonably sized adaptive antennas cannot completely alleviate this problem. Specifically, there are cases where the positions of the victim and interfering base stations are such that the antenna array would be required to form a beam along the array element axis. Forming a narrow endfire beam with a practical number of elements is very difficult.

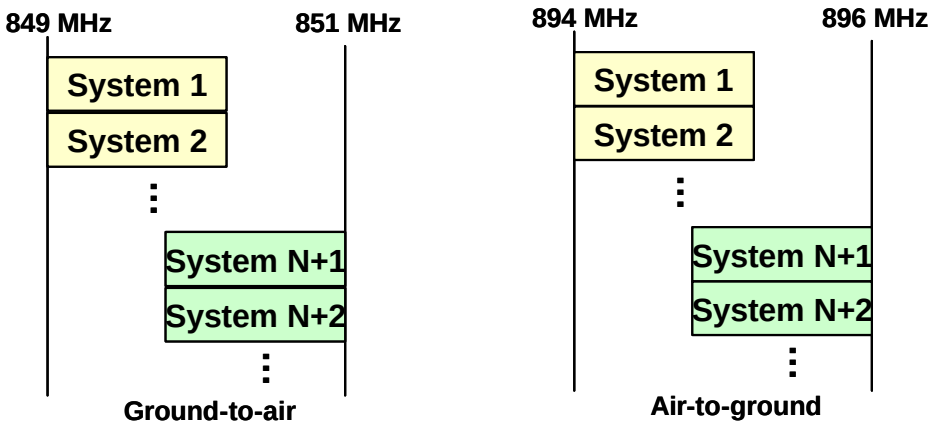

Figure 41: *Proposed spectral sharing plan.*

Finally, the complexity of the proposed adaptive antenna system is much greater than Airfone's proposed switched-beam system. This increased complexity will lead to greater size, weight, and power consumption requirements for the same number of antenna elements, and therefore would not be practical for an ATG service. Aviation customers are extremely concerned about any one of these elements when introducing new technology to their aircraft fleet. With all these factors adversely affected by an adaptive array system, such a design would not be acceptable in the commercial aviation marketplace. Also, commercial off-the-shelf adaptive array systems do not currently exist for air-to-ground broadband communications applications, and the required engineering and testing necessary to develop such a complex system would lead to significant time-to-market delays.

6.2. System Layout

Boeing has proposed interleaving base stations of competing systems so that system #2 base stations would be placed some minimum distance from system #1 bases stations. They propose that this type of arrangement can be used to accommodate up to 6 competing providers. An example of this proposed layout with two providers is shown in Figure 42.

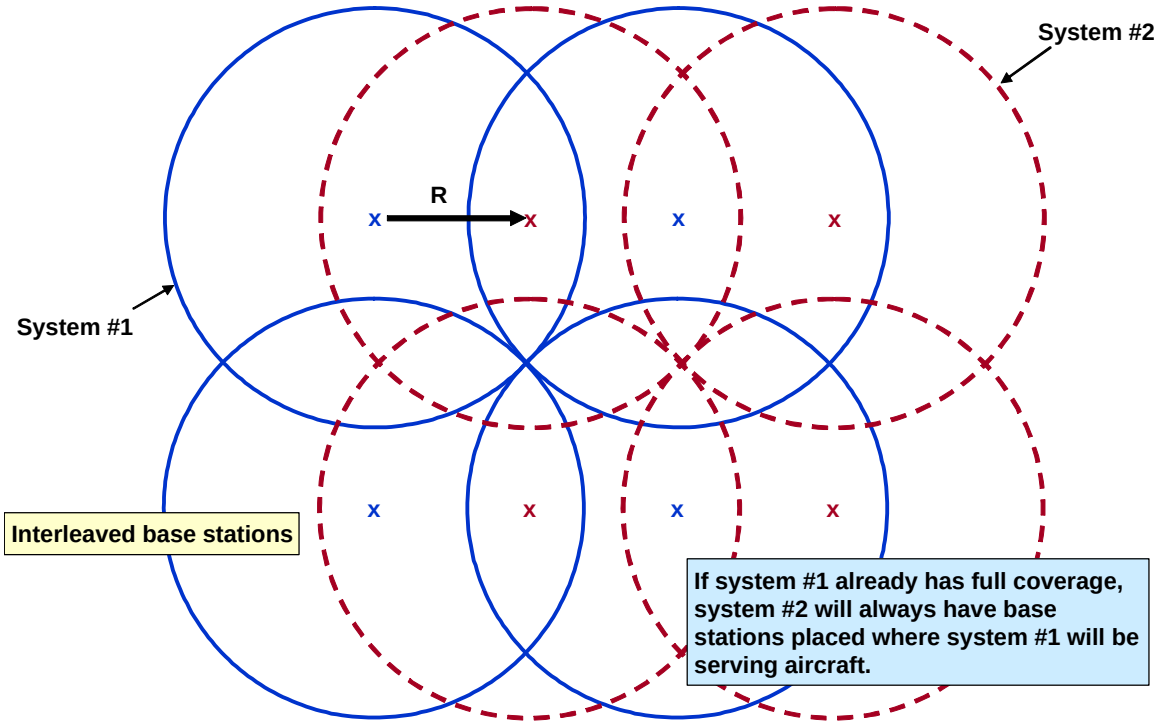

Figure 42: *Example of interleaved base station layout with two competing providers.*

One observation is that system #2 base stations are placed where signals from system #1 base stations are weakest, creating severe interference problems. Considering the ground-to-air link, without significant antenna discrimination between the two opposing system's base stations, system #1 aircraft would see a very large signal from system #2 base stations and weak signals from their own base stations. An idealized plot of the signal strength from each base station is shown in Figure 43. If we consider the air-to-ground link, base stations from system #1 could have aircraft belonging to system #2 very close to them while trying to communicate with their own aircraft that are very far away (classic near-far problem).

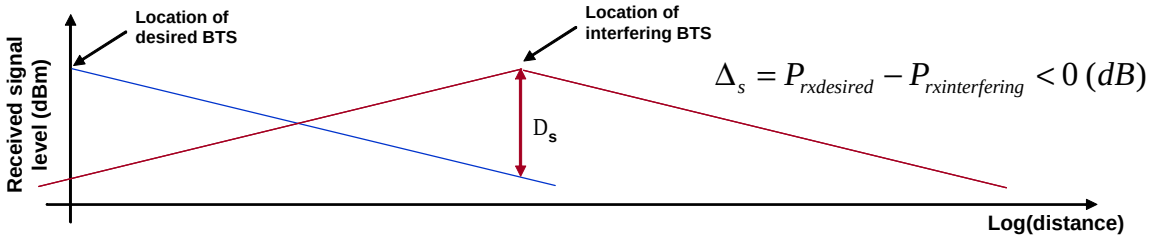

Figure 43: *Idealized plot of received signal from base stations of two interfering systems.*

6.3. Antenna Size Considerations

The only way to deal with the kind of interference problem discussed in the previous section is to install adaptive antennas on both ends of the link. These antennas can form beams which aim at the desired base station or aircraft, while attenuating the signal from the interfering base station through pattern roll-off or nulls. As we will see however, for cases where interfering and desired base station are not separated by reasonable angles, a prohibitively high number of antenna elements is required to form a beam that is narrow enough to aim at the desired base station, while attenuating the interferer. These cases occur where the serving base station is angularly very close to an interfering base station. This can frequently occur in the vicinity of airports when both systems have base stations near the airport and in edge-of-network areas, such as coastal regions.

An example that creates such an interference problem that is difficult to alleviate with an adaptive array is shown in Figure 44. In this scenario, the two interfering base stations are co-aligned and can only be distinguished in the elevation direction.

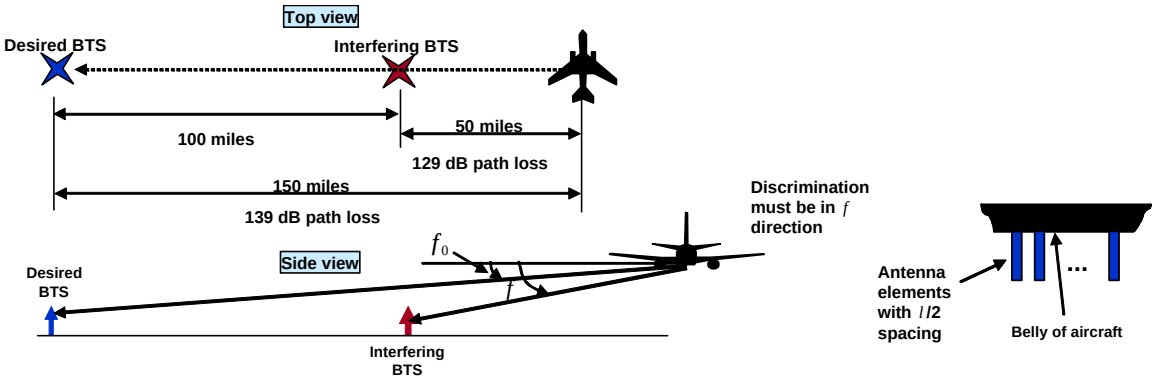

Figure 44: *Worst-case situation for adaptive array system to distinguish opposing base stations.*

In this admittedly worst case scenario, the victim aircraft is 50 miles from an interfering base station, but 100 miles from the desired base station. This results in a 10 dB path loss difference in favor of the interfering base station, i.e., the signal from the interfering base station is 10 dB higher than the signal from the desired base station. In order to reach just

a 0 dB SINR, the antenna discrimination must be such that the interfering signal is attenuated by 10 dB with respect to the desired base station. Both of these base stations are aligned in azimuth from the perspective of the aircraft. This implies that we cannot use the azimuthal discrimination provided by the belly-mounted array. Since the array is belly-mounted, the beam that must be formed to discriminate in elevation is near endfire.

The gain of the belly-mounted uniformly illuminated, equally spaced ($l/2$ element spacing) array with respect to boresight pointing angle f_0 and elevation angle f, with angles oriented as shown in Figure 44, is

$$G(f;N)=\frac{\sin\left(N\left\{p\left(\cos f-\cos f_0\right)\right\}/2\right)}{N\sin\left(\left\{\cos f-\cos f_0\right\}/2\right)} \tag{12}$$

For the geometry shown in Figure 44, the angle to the interferer is $f=8^\circ$ and the angle to the desired base station is $f_0=3^\circ$. To provide the required antenna discrimination, we aim the beam toward the desired base station and need to determine the number of elements *N* that are necessary to obtain -10 dB of gain in the direction of the interferer. It is found that 190 elements along the dimension parallel to the wings is required. Also, since this discrimination would be required regardless of the heading of the aircraft, the array should be a square array, requiring 190^2=36,100 elements. This array would be 100 feet on a side at 895 MHz and would require 36,100 receiver chains. An example of two antenna patterns with 20 and 200 elements is shown in Figure 45.

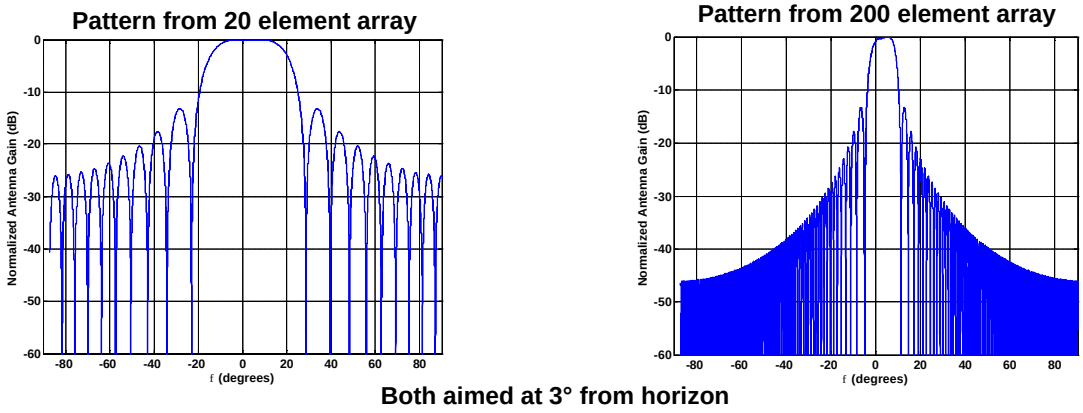

Figure 45: *Example antenna array patterns for 20 element and 200 element arrays.*

It may be possible to use a non-uniform weighting of the elements or a non-uniformly spaced array, but the absurd number of elements required show that it is clearly very difficult to form a narrow enough beam to attenuate a near co-linear interfering base station using a belly mounted array. We also acknowledge that it is possible, in very high

SNR environments, to find weights for an adaptive array that could permit attenuation of the interferer without the half-beam spacing between interferer and desired base stations as discussed above. However, in the ATG situation, the full beam gain will be used to complete the link and we will not have the latitude to permit the closer spacing, i.e., we will not be able to reduce the number of required elements.

It can be argued that this example is extreme and that this case may not be encountered frequently in the real-world. We will therefore consider a situation that is likely to occur in reality. Shown in Figure 46 is a map of the area surrounding Chicago's O'Hare International airport. Since there are many aircraft to serve in the area, Airfone currently has two base station installations around the airport to handle the demand. It is likely that another provider would install a similar number of base stations near the airport. We shall assume that they are as far from system #1 base stations as possible while still being located very near the airport.

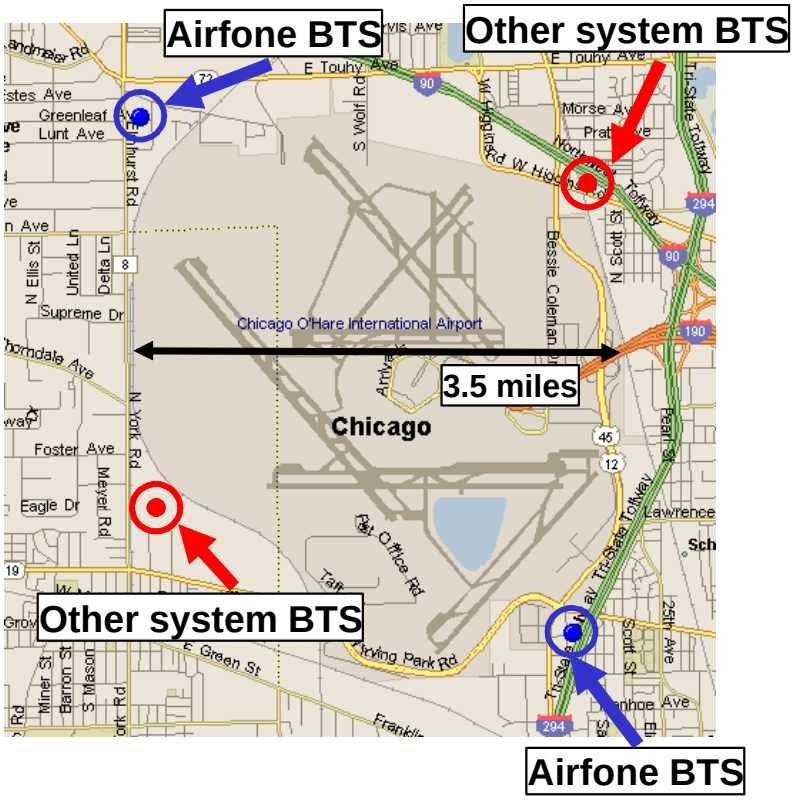

Figure 46: *Two system scenario near Chicago's O'Hare International Airport.*

Since, as aircraft fly near and into the airport for the case shown in the figure, the base stations will not typically be aligned, the antenna system can now rely on azimuthal separation to distinguish interfering from desired base stations. A simple simulation was performed to determine the maximum azimuth angle separation between desired and interfering base stations. This maximum angular separation can be used to determine the required number of elements to obtain some level of antenna discrimination. Here, since

the base stations are all at essentially the same distance from the aircraft when the aircraft is far from the airport, the SINR will be approximately -5 dB without antenna discrimination (3 interferers and 1 desired signal all at the same level). As a rough approximation, we will assume that we need about 3 dB of discrimination, bringing the SINR to -2 dB.

The approximate formula for half-power beamwidth for a near-broadside uniformly excited equally spaced array is given by [10] to be

$$HP \approx 0.886 \frac{l}{Nd} \csc q_0, \tag{13}$$

where q_0 is the beam pointing angle, which will be considered to be the best case here at $q_0 = 90^\circ$. This expression can be used to relate half-power beamwidth to the required number of elements *N*.

The simulation developed here moves the aircraft around the airport in 10° steps through 360° at a fixed distance. Pointing angles to each base station are found for each angular position at the given distance and the maximum angular separation between interfering and desired base station is then chosen for that distance. This is a best case assumption, since there will be many angular positions around the airport at that distance where the azimuthal separation between desired and interfering base stations will be smaller.

A plot showing maximum azimuthal separation and required number of elements is shown in Figure 47. It can be seen that as the aircraft is further from the airport, all of the base stations appear to be co-located (small angular separation), thus requiring a large array to discriminate base stations. This means that it is very difficult to aim a beam at the desired base station without also aiming it at the interfering base stations. Similarly, it is difficult to point a null at the interferers without pointing that same null at the desired base stations.

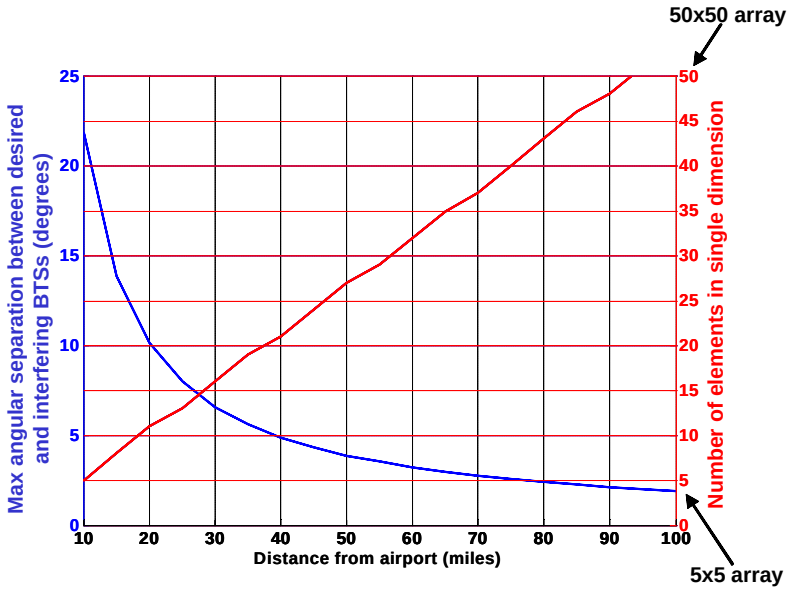

Figure 47: *Angular separation and number of required elements versus distance from airport.*

6.4. System Complexity Considerations

If it were possible to alleviate all of the possible interference problems associated with the sharing of spectrum with a reasonably sized array, the complexity, cost, and power consumption associated with a fully adaptive array become excessive compared to a switched-beam system.

Figure 48 shows a block diagram of an *N*-beam switched-beam system. A Butler matrix is used to form the *N* beams and a second "scanning" receiver is used to monitor all beams for the best SINR. When the scanning receiver finds the best beam, it commands the main beam *N*-way switch to move to the proper beam. This approach requires 2 *N*-way switches, a Butler matrix and two receive chains.

Figure 49 shows a block diagram of an *N*-element adaptive antenna system. *N* receive chains and an adaptive weight processor are necessary. Since the receiver chains are probably the most expensive part of each design, the adaptive antenna approach is more expensive. Also, the receive chains contain active components. Therefore, the adaptive antenna design will likely consume more power.

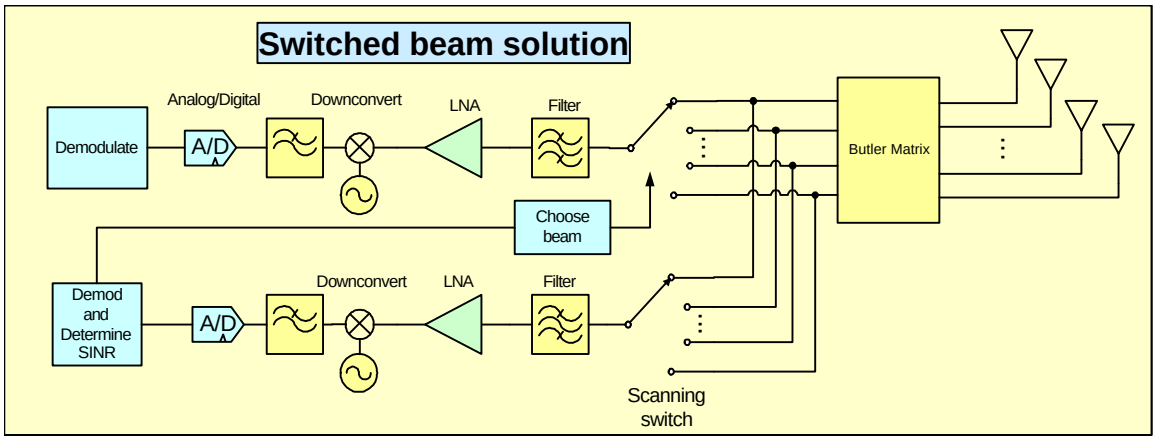

Figure 48: *Switched beam system block diagram.*

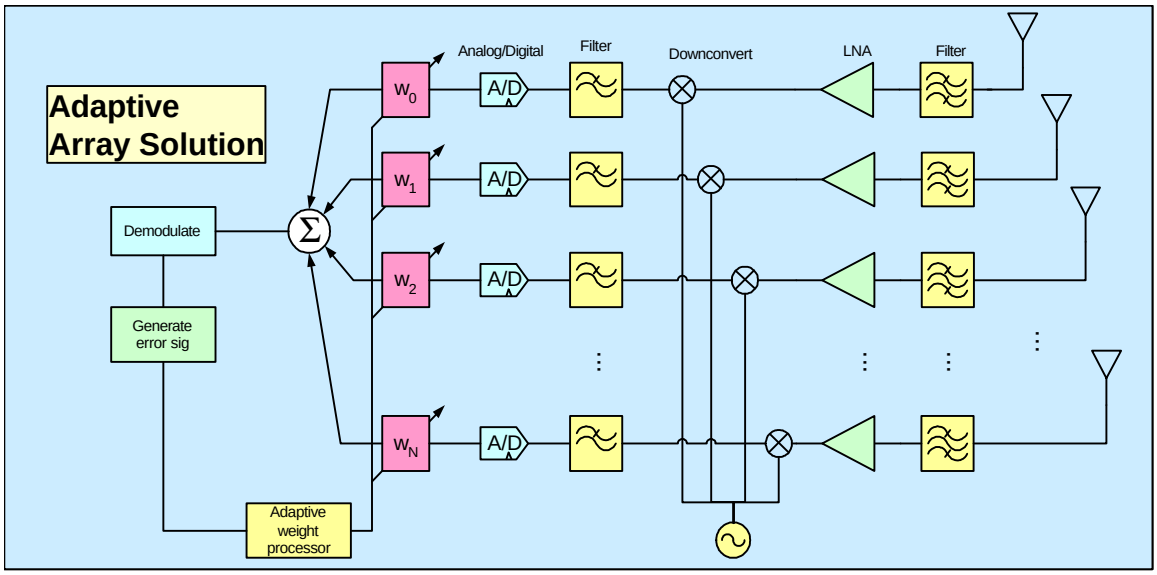

Figure 49: *Adaptive antenna system block diagram.*

Another thing to note is that since the adaptive antenna approach is much more complex, the development and testing effort for such a system is much greater that that for the switched-beam system. This added design and testing time will result in additional time-to-market delays.

6.5. Conclusions

For the proposed spectrum sharing plan where multiple providers overlap within the same spectrum (not cross-duplexed), several scenarios presented here illustrate the difficulty associated with discriminating between multiple providers during signal reception. When the serving and interfering base stations are not well separated angularly, an adaptive antenna will find it difficult to attenuate the interferer. The only way to accomplish the

required attenuation is to use an unreasonably large and expensive array to achieve the required narrow beam widths. Even for moderately sized arrays (5x5), the required design, system engineering, and flight testing of these arrays would lead to increased cost, weight, power consumption (over a switched beam system) and time-to-market delays. With all these factors considered, any adaptive array design similar to the type proposed by Boeing would fail to be commercially viable for the ATG spectrum.

7. Annex A: The Radio Horizon

Figure 50 shows the geometry for calculating the radio horizon $d_{\max}$ as a function of the elevation *h* of an antenna above the surface of the Earth. If *r* is the effective Earth radius, including correction for diffraction, then

$$\begin{aligned} d_{\max} &= \sqrt{(r+h)^2 - r^2} \\ &\cong \sqrt{2rh}\,, \quad h << r \end{aligned} \tag{14}$$

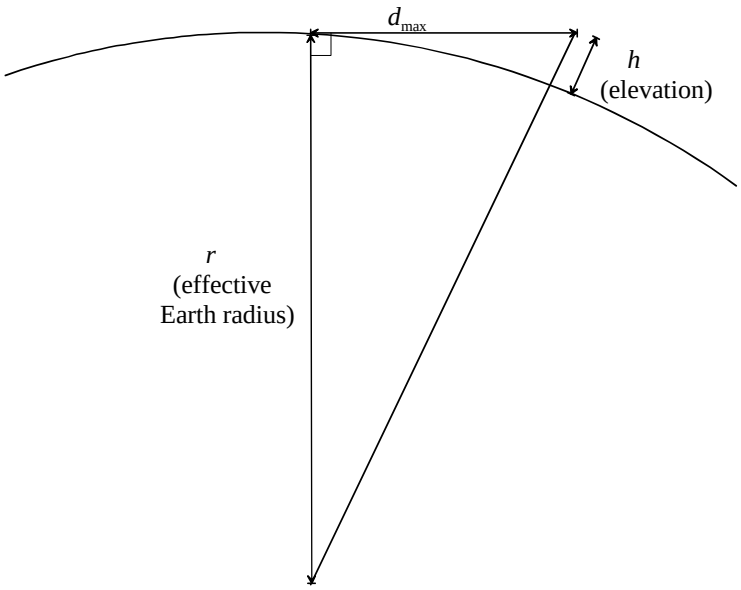

Figure 50: *Geometry for computing the radio horizon.*

For the standard diffraction correction factor $K = 4/3$, $r = 5{,}328\,\text{mi}$. Therefore, if *h* is expressed in feet, (14) becomes:

$$d_{\max} \cong \sqrt{2h}\,, \quad h << 28\times10^6\,\text{ft} \tag{15}$$

where $d_{\max}$ is in miles and h is in feet. By extension, the radio horizon between two points with elevations h_1 and h_2 above the Earth's surface is

$$d_{\max} \cong \sqrt{2}\left(\sqrt{h_1} + \sqrt{h_2}\right). \tag{16}$$

8. Annex B: Reverse Link Capacity and Load Factor

Let I_{tot} be the total noise plus interference at the base station receiver, *W* be the signal bandwidth, and P_j and R_j be the receive signal power and date rate, respectively, for the j^{th} mobile in the cell or sector. Letting E_b and N_t represent the received energy per bit and the power spectral density of the noise plus interference (that is I_{tot}/W), then the noise plus interference as seen by the receive channel unit associated with the j^{th} mobile is $I_{tot} - P_j$ and:

$$\left(\frac{E_b}{N_t}\right)_j = \frac{P_j W/R_j}{I_{tot} - P_j} \tag{17}$$

Defining the "jamming margin" as

$$M_j \equiv \frac{W/R_j}{(E_b/N_t)_{\min,\, j}}, \tag{18}$$

(17) gives

$$I_{tot} \le P_j(M_j + 1) \tag{19}$$

Let *N* be the (thermal) receiver noise, $I_{in} = \sum_j P_j$ is the total received signal power due to in-cell (or in-sector) mobiles, and I_{oc} be the interference from mobiles associated with other cells or sectors. Generally, $I_{oc} = fI_{in}$ where the factor *f* depends on propagation parameters. With these parameters,

$$I_{tot} = N + (1+f)I_{in} = N + (1+f)\sum_j P_j \tag{20}$$

If there are *K* users per cell or sector with equal rates and E_b/N_t requirements, and the power received from each is *P*, then $I_{in} = KP$ and (20) becomes

$$I_{tot} = N + KP(1+f) \tag{21}$$

Letting *M* denote the jamming margin, which is now the same for all users, combining (19) becomes $I_{tot} = P(M+1)$ and (21) is

$$N + KP(1+f) = P(M+1) \tag{22}$$

Letting $N = 0$ gives the pole capacity as

$$K_{pole} = \frac{M+1}{1+f} \tag{23}$$

Rearranging (22) gives

$$K = \frac{P(M+1) - N}{P(1+f)} = K_{pole} - \frac{N}{P(1+f)} \tag{24}$$

or

$$\frac{P(1+f)}{N} = \frac{1}{K_{pole} - K} \tag{25}$$

Multiplying both sides by K_{pole} and using $I_{tot} = P(M+1)$ from (21) and (22) gives

$$\frac{I_{tot}}{N} = \frac{1}{1 - K/K_{pole}} \tag{26}$$

which defines the CDMA reverse link load curve shown in Figure 51. Note also that if N_0 is the thermal noise power spectral density, then $N_t / N_0 = I_{tot} / N$.

From (26) the received signal power at the base station is

$$P = \frac{I_{tot}}{M+1} = \frac{N}{(1 - K/K_{pole})(M+1)} \tag{27}$$

or in dBm

$$P = N + F_{load} - M_J \tag{28}$$

where $F_{load} = -10\log(1 - K/K_{pole})$ and $M_J = 10\log(M+1)$. For $M >> 1$, $M_J \cong 10\log M$.

The AirCell Reverse Link Pole Point Analysis

In eq. (6) of its analysis (p. 22), AirCell [3] gives the equation (expressed in the notation introduced above):

$$\left(\frac{E_b}{N_t}\right)_j = \frac{P_j W/R_j}{\sum_{i \neq j} P_i(1+f)+N} \tag{29}$$

It follows that with this model, $I_{tot} = N + (K-1)P(1+f) + P = N + KP(1+f) - Pf$, which seems to be an error on AirCell's part. With $I_{tot} = P(M+1)$, this gives

$$N + KP(1+f) - Pf = P(M+1) \tag{30}$$

and setting $N = 0$ gives the pole capacity as

$$K_{pole} = \frac{M+1+f}{1+f} \tag{31}$$

Rearranging (30) and substituting (31) gives

$$K = \frac{P(M+1+f)-N}{P(1+f)} = K_{pole} - \frac{N}{P(1+f)} \tag{32}$$

Hence,

$$\frac{P(1+f)}{N} = \frac{1}{K_{pole} - K} \tag{33}$$

and multiplying by K_{pole} gives

$$\frac{P(M+1+f)}{N} = \frac{1}{1-K/K_{pole}} \tag{34}$$

or, since $I_{tot} = P(M+1)$,

$$\frac{I_{tot}+Pf}{N} = \frac{1}{1-K/K_{pole}} \tag{35}$$

Thus, $P = \frac{N}{(1-K/K_{pole})(M+1+f)}$ and (28) also applies if $M >> 1$ and $M >> f$. However, it is unclear if this is the relationship that AirCell used to calculate the required received power from each aircraft (and hence its transmitted power).

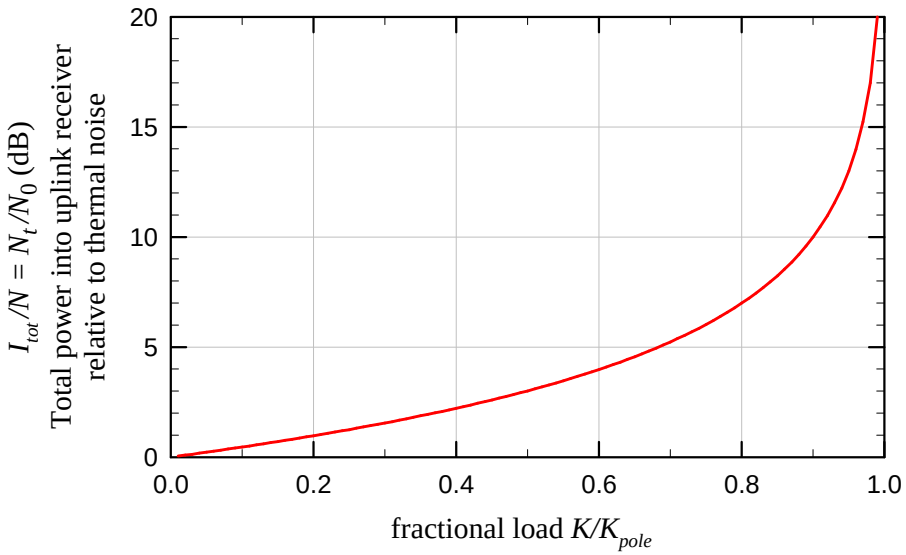

Figure 51: *CDMA reverse link load curve*

9. Annex C: Analytical Approximation of the SIR Using Circular Geometry

While simulations are widely used to study complex situations, they often fail to provide the physical insights necessary to understand key relationships and factors that are most important in determining results. It is therefore often useful to construct, in addition to the simulations, a simplified analytical model that can show key relationships explicitly, and can also be used to validate the simulation results for selected cases. This Annex develops such a model for the SIR and compares the results to those from the square grid simulation discussed above.

With this model, a cell coverage area is represented as a circle of radius r_c centered on the base station. Free space propagation is assumed, altitude is ignored, and base station antenna gain is assumed constant, independent of the location of the aircraft. As will be seen, making these simplifying assumptions makes little difference in the end results, while providing insights into the dominant relationships.

Model Development

With this simplified model, there are three factors that determine the SIR seen by the receiver on the aircraft: (1) the path loss between the interfered aircraft and its base station; (2) the path loss between the interfered and interfering aircraft; and (3) the power transmitted by the interfering aircraft. Each of these three factors can be represented by a random variable with a uniform distribution, which can be seen as follows.

Consider two concentric circles of radii $d_{\min}$ and $d_{\max}$. If a point is randomly located, uniformly over area, in the area between these circles, the probability density function (PDF) of the distance between the point and the center is

$$f_d(r) = \frac{2r}{d_{\max}^2 - d_{\min}^2} \qquad d_{\min} \le r \le d_{\max} \tag{36}$$

and the cumulative distribution function (CDF) is

$$\Pr(d < r) = \frac{r^2 - d_{\min}^2}{d_{\max}^2 - d_{\min}^2}. \tag{37}$$

The free space path loss between the center and the point at distance *r* is

$$L(d) = k_{pl} d^2 \tag{38}$$

Hence, the CDF of the path loss is

$$\begin{aligned}\Pr\left(L_p < L\right) &= \Pr\left(k_{pl} d^2 < L\right) \\ &= \Pr\left(d < \sqrt{\frac{L}{k_{pl}}}\right) = \frac{L - L_{\min}}{L_{\max} - L_{\min}}\end{aligned} \tag{39}$$

where $L_{\min} = k_{pl} d_{\min}^2$ and $L_{\max} = k_{pl} d_{\max}^2$. The corresponding PDF is uniform between $L_{\min}$ and $L_{\max}$:

$$f_{L_p}(L) = \frac{1}{L_{\max} - L_{\min}}, \qquad L_{\min} \le L \le L_{\max}. \tag{40}$$

This general expression applies to both the distance from the interfered aircraft to its base station, and the distance between the interfered and interfering aircraft.

Assuming the interfering aircraft has perfect power control on the reverse link, its transmitted power is proportional to the path loss to its controlling base. Therefore, the CDF of the EIRP from the interfering aircraft is:

$$\Pr\left(EIRP_{AC} < P\right) = \frac{P - EIRP_{AC,\min}}{EIRP_{AC,\max} - EIRP_{AC,\min}} \tag{41}$$

and the corresponding PDF is uniform:

$$f_{EIRP_{AC}}(P) = \frac{1}{EIRP_{AC,\max} - EIRP_{AC,\min}}, \qquad EIRP_{AC,\min} < P < EIRP_{AC,\max} \tag{42}$$

Note that if the transmit EIRP is expressed in dBm, the CDF is

$$\begin{aligned}\Pr\left(10\log EIRP_{AC} < P_{dB}\right) &= \frac{10^{P_{dB}/10} - EIRP_{AC,\min}}{EIRP_{AC,\max} - EIRP_{AC,\min}} \\ &= \frac{e^{P_{dB}\ln 10/10} - EIRP_{AC,\min}}{EIRP_{AC,\max} - EIRP_{AC,\min}}, \quad 10\log EIRP_{AC,\min} \le P_{dB} \le 10\log EIRP_{AC,\max}\end{aligned} \tag{43}$$

and the PDF is exponential:

$$f_{10\log EIRP_{AC}}(P_{dB}) = \frac{\ln 10}{10} \cdot \frac{e^{P_{dB}\ln 10/10}}{EIRP_{AC,\max} - EIRP_{AC,\min}}, \quad 10\log EIRP_{AC,\min} \le P_{dB} \le 10\log EIRP_{AC,\max} \tag{44}$$

Normalization

In general, there will be some number *K* of interfering aircraft within the radio horizon of the interfered aircraft. Let $EIRP_{TX,k}$ and $L_{AC,k}$ be, respectively, the EIRP of the k^{th} interfering aircraft and its path loss to the victim aircraft. The total interference to the victim aircraft is then

$$I_{AC} = \sum_{k=1}^{K} \frac{EIRP_{TX,k}}{L_{AC,k}} \tag{45}$$

Normalized versions of $EIRP_{TX,k}$ and $L_{AC,k}$ can be defined as:

$$x_k = \frac{EIRP_{TX,k}}{EIRP_{AC,\max}}, \quad y_k = \frac{L_{AC,k}}{L_{AC,\max}} \tag{46}$$

The PDFs of x_k and y_k are:

$$f_{x_k}(x) = \frac{1}{1 - x_{\min}} \qquad x_{\min} \le x \le 1$$
$$f_{y_k}(x) = \frac{1}{1 - y_{\min}} \qquad y_{\min} \le y \le 1 \tag{47}$$

where

$$x_{\min} = \frac{EIRP_{AC,\min}}{EIRP_{AC,\max}}, \quad y_{\min} = \frac{L_{AC,\min}}{L_{AC,\max}} \tag{48}$$

Thus, letting

$$\begin{aligned} z_k &= \frac{x_k}{y_k} \\ z_K &= \sum_{k=1}^{K} z_k \end{aligned}, \tag{49}$$

It follows that

$$I_{AC} = \frac{EIRP_{AC,\max}}{L_{AC,\max}} z_K . \tag{50}$$

Similarly, letting L_B represent the path loss between the interfered aircraft and its base station, and $EIRP_B$ be the EIRP of the base station, the received desired signal power is

$$S = \frac{EIRP_B}{L_B} \tag{51}$$

Defining the normalized path loss as

$$y_B = \frac{L_B}{L_{B,\max}}, \tag{52}$$

its PDF is

$$f_{y_B}(y) = \frac{1}{1 - y_{B,\min}}, \qquad y_{B,\min} \le y \le 1. \tag{53}$$

Besides interference from other-system aircraft, the aircraft will also sustain interference from outer-cell base stations of its own system. This interference is denoted I_{oc}. The total signal to interference ratio is then:

$$SIR = \frac{EIRP_B}{L_{B\max} y_B} \cdot \frac{1}{\dfrac{EIRP_{AC,\max}}{L_{AC,\max}} z_K + I_{oc}} \tag{54}$$

For a cell surrounded on all sides by other cells, the outer cell forward link interference varies relatively little with the location of the aircraft, compared to desired signal, and is approximated as a constant for purposes of this simplified model. Thus,

$$I_{oc} = b \, \frac{EIRP_B}{L_{B,\max}} \tag{55}$$

that is, the outer-cell interference is some factor b times the received desired signal at the cell edge.

The interference-to-signal ratio (ISR) is therefore

$$\begin{aligned} ISR &= y_B \, \frac{L_{B,\max}}{EIRP_B} \left(\frac{EIRP_{AC,\max}}{L_{AC,\max}} z_K + b \, \frac{EIRP_B}{L_{B,\max}} \right) \\ &= y_B \left(\frac{L_{B,\max} EIRP_{AC,\max}}{L_{AC,\max} EIRP_B} z_K + b \right) \\ &= y_B \left(K_{ISR} \, z_K + b \right) \end{aligned} \tag{56}$$

where $K_{ISR} = \dfrac{L_{B,\max} EIRP_{AC,\max}}{L_{AC,\max} EIRP_B}$, and $SIR = \dfrac{1}{ISR}$.

The component random variables y_B, x_k, and y_k can be easily generated numerically.

To calculate the parameters $L_{AC,\max}$, $L_{B,\max}$, and $EIRP_{AC,\max}$, the "cell" is assumed to be a circle of radius r_c, and all of the maximum path losses will be based on this distance. In the case of the aircraft-to-aircraft path loss, the actual maximum path loss would correspond to the radio horizon, but far-away aircraft contribute little to the total interference, and only interfering aircraft within one cell radius of the interfered aircraft will be included in the interference calculation.

In that case, the parameters in decibel units are

$$L_{B,\max} = L_{AC,\max} = 95.3 + 20 \log r_c \quad \text{dB} \tag{57}$$

$$EIRP_B = P_{B,TX} + G_{B\max} - L_{cabl} - L_{dipl} - M_{sys} \text{ dBm} \tag{58}$$

$$\begin{aligned} EIRP_{AC,\max} &= -17.7 + F_{noise} + F_{load} - M_J + F_{ckts} \\ &\quad - G_{B\max} + L_{cabl} + L_{dipl} + M_{sys} + 20\log r_c \text{ dBm} \end{aligned} \tag{59}$$

Thus,

$$\begin{aligned} 10\log K_{ISR} = 10\log\left(\frac{EIRP_{AC,\max}}{EIRP_B}\right) &= -17.7 + 2\left(L_{cabl} + L_{dipl} + M_{sys} - G_{B\max}\right) \\ &\quad - P_{B,TX} + F_{noise} + F_{load} - M_J + F_{ckts} + 20\log r_c \end{aligned} \tag{60}$$

In the simulation, the cell is a $D \times D$ square. For the circular cell to have the same area, $r_c = D/\sqrt{p}$, which is 112.8 miles for $D = 200$ miles as was assumed in the simulation. For the parameter values used previously ($P_{BTX} = 43$ dBm, $L_{cabl} = 3$ dB, $L_{dipl} = 2$ dB, $G_{B\max} = 9$ dB, $F_{load} = 6$ dB, $F_{noise} = 5$ dB, $M_J = 17$ dB, and $M_{sys} = 10$ dB) with $F_{ckts} = 10$ dB and $r_c = 112.8$ miles, the base station and aircraft maximum EIRP levels are $EIRP_B = 37$ dBm and $EIRP_{AC,\max} = 33.35$ dBm, so $10\log K_{ISR} = -3.65$.

If the OCI is roughly a factor of 3 above the desired signal at the corner of a square cell, then:

$$b \cong 3 \times \left(\frac{r_c\sqrt{2}}{D}\right)^2 = \frac{6}{p} = 1.9. \tag{61}$$

Results

Figure 52 shows the forward link capacity and outage probability for $10\log K_{ISR} = -3.65$ and $b = 1.9$, using the approximation, and Figure 53 shows the results for $b = 1$. Note the close agreement with Figure 19.

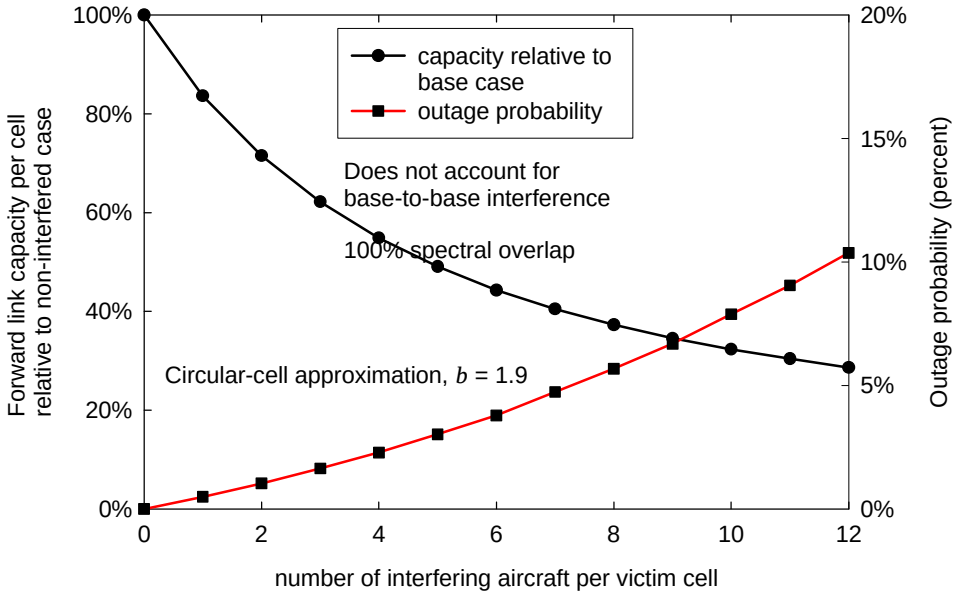

Figure 52: *Effect of cross-duplex interference, based on circular-cell approximation.* $b = 1.9$.

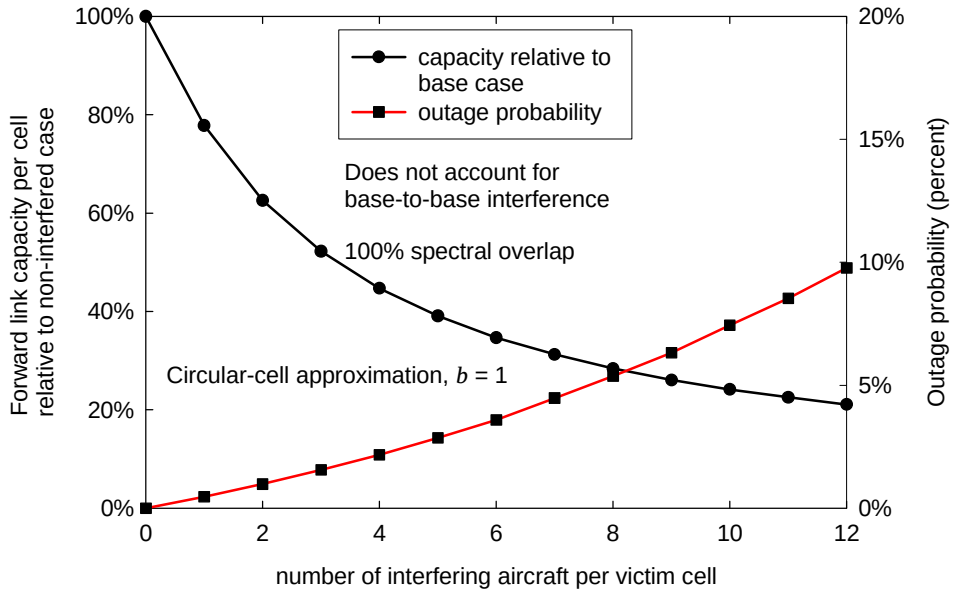

Figure 53: *Effect of cross-duplex interference, based on circular-cell approximation.* $b = 1.0$.

To summarize, the simple analytical model developed here allows the SIR to be expressed as

$$SIR = \frac{EIRP_B}{EIRP_{AC,\max}} \frac{1}{y_B} \left(\frac{1}{z_K + b \dfrac{EIRP_B}{EIRP_{AC,\max}}} \right) \tag{62}$$

which shows that the dominant factor in determining the impact on the SIR is the ratio of the base station EIRP to the maximum aircraft EIRP (given the aircraft density).

Figure 54 and Figure 55 show the CDFs for the SIR with 3 and 12 interfering aircraft per cell, respectively. Note that for these cases, there is relatively little sensitivity to the outer cell interference factor b. These curves are shown on a Gaussian scale (on which a Gaussian distribution would appear as a straight line), so at least for the cases shown, the SIR might reasonably be approximated as lognormal.

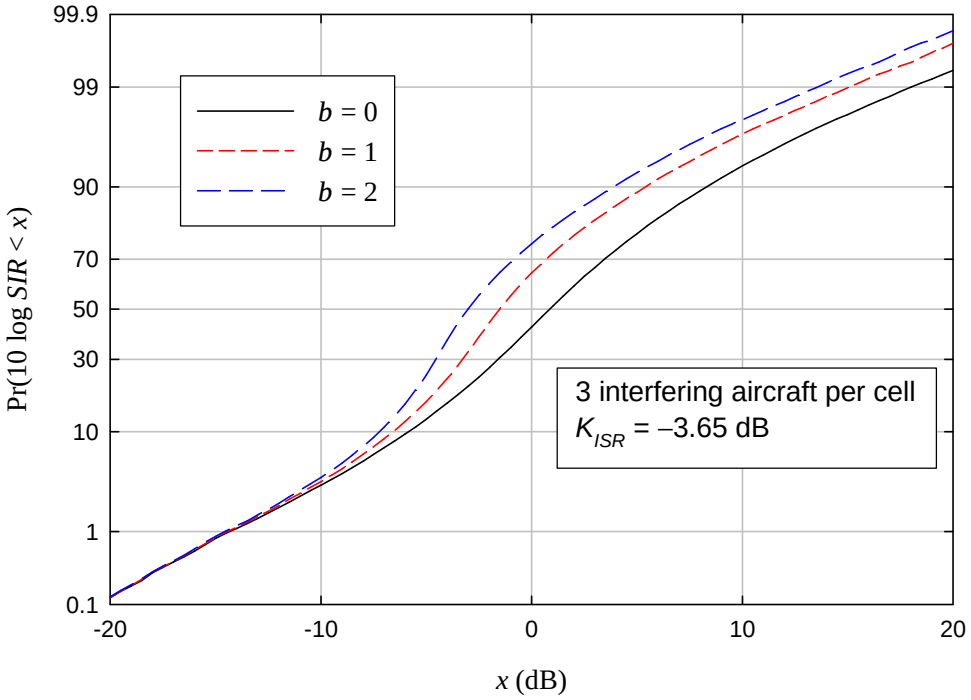

Figure 54: *CDF of the SIR for 3 interfering aircraft per cell.*

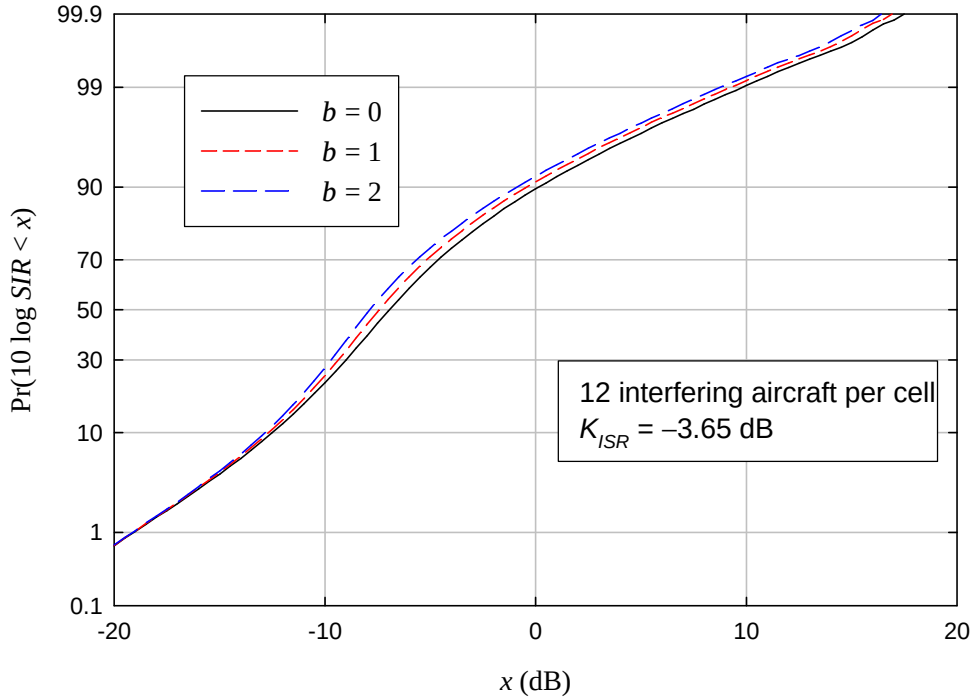

Figure 55: *CDF of the SIR for 12 interfering aircraft per cell.*

Since y_B is the normalized path loss from the desired base station to the victim aircraft, the statistics of the SIR can be studied over a limited part of the cell coverage area by changing the limits on y_B . For example, to determine the outage probability for aircraft on the outermost 20% of the cell area, the minimum value of y_B corresponds to the path loss at a distance of $\sqrt{0.8}r_c$. Since free space path loss varies as the square of distance, $y_{B\min} = 0.8$ in this case. Figure 56 shows the outage probability vs. the number of interfering aircraft per cell for different outermost percentages of the cell coverage area. As would be expected, the outermost areas of the cell are the most strongly affected by the cross-duplex interference.

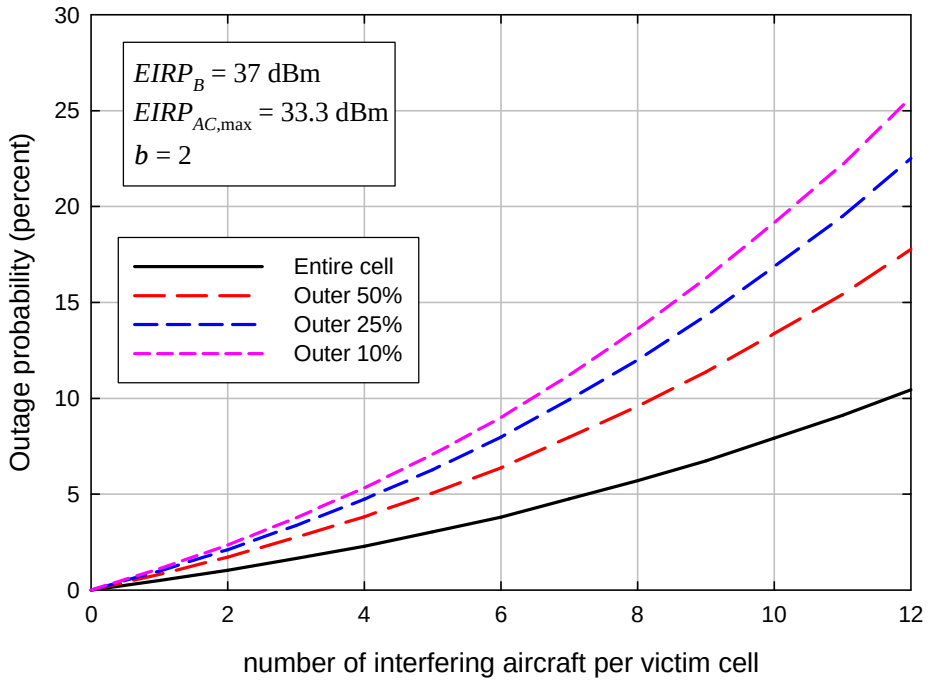

Figure 56: *Outage probabilities for different outermost fractional cell areas.*

This Annex has shown that the effect of the aircraft-to-aircraft interference in cross-duplexed ATG systems can be determined using single-cell model, representing the cell boundary as a circle and the outer-cell (same system) interference as a constant. The path loss between the victim aircraft and its desired base station, the power transmitted by each interfering aircraft, and the path loss between each interfering aircraft and the victim aircraft are represented as uniformly-distributed random variables. When these random variables are normalized it becomes clear that the main factors that determine the effect of the cross-duplex interference are the EIRP of the desired base station and the maximum EIRP of the interfering aircraft, as well as the number of aircraft per cell.

10. References

[1] Verizon Airfone Presentation to the FCC, December 3, 2003 WT Docket 03-103.

[2] AirCell Presentation to the FCC, January 14, 2004, WT Docket 03-103.

[3] AirCell report to the FCC "Evaluation of the ATG Spectrum Migration Concept," Ivica Kostanic and Dan McKenna, March 10, 2004, WT Docket 03-103.

[4] Private communications with Verizon Airfone.

[5] P. Bender, *et al*, "CDMA/HDR: A Bandwidth-Efficient High-Speed Wireless Data Service for Nomadic Users," *IEEE Communications Magazine*, July 2000, pp. 70-77.

[6] AirNav Systems, LLC, Dallas, TX, *Live Flight Tracker 2* Software.

[7] Clark, J.P. and Evans, A.D., "A Case Study of Delays and Response Strategies at Newark Airport", Proceedings of Workshop on Airline and National Strategies for Dealing with Airport and Airspace Congestion, University of Maryland, March 15-16, 2001.

[8] Aircraft movement data for 2001 available from the Airports Council International at http://www.airports.org.

[9] M.I. Skolnik, *Introduction to Radar Systems*, New York, NY, McGraw-Hill, 1980.

[10] Stutzman, W.L. and Thiele, G.A., Antenna Theory and Design, New York, Wiley & Sons, 1981.

[11] Boeing Presentation to the FCC, March 1, 2004, WT Docket 03-103.

[12] FCC Public Notice, DA 98-2394, November 25, 1998, pp. 3-6.

[13] "Output Tube Emission Characteristics of Operational Radars." R. J. Matheson, *et al*, NTIA Report 82-92, January, 1982.